NASA-CR-172335
19840015540

NASA CONTRACTOR REPORT 172335

FURTHER DEVELOPMENT OF XTRAN3S COMPUTER PROGRAM

C. J. BORLAND
BOEING MILITARY AIRPLANE COMPANY
SEATTLE, WASHINGTON 98124

CONTRACT NAS1-17072

MAY 1984

National Aeronautics and
Space Administration

Langley Research Center
Hampton, Virginia 23665

1 Report No.	2. Government Accession No.	3. Recipient's Catalog No.
NASA CR-172335		

4 Title and Subtitle	5. Report Date
Further Development of XTRAN3S Computer Program	May 5, 1984
	6. Performing Organization Code

7. Author(s)	8. Performing Organization Report No.
C. J. Borland	
	10. Work Unit No.

9. Performing Organization Name and Address	11. Contract or Grant No.
Boeing Military Airplane Company P.O. Box 3707 Seattle, Washington 98124	NAS1-17072
	13. Type of Report and Period Covered Contractor Report

12. Sponsoring Agency Name and Address	14. Sponsoring Agency Code
National Aeronautics and Space Administration Washington, DC 20546	

15. Supplementary Notes

Langley Technical Monitor: Robert M. Bennett
Final Report--September 10, 1982 - February 10, 1984

16. Abstract

This report describes modifications and enhancements to XTRAN3S, a computer program for aerodynamic, static aeroelastic, and dynamic aeroelastic analysis of three-dimensional wings in the transonic speed regime. Modifications to the program include incorporation of a viscous boundary layer, modified coefficient and generalized force integration, direct input of airfoil surface coordinates and slopes, variable dimensions of computational arrays and a modified grid mapping transformation to improve computational stability for highly swept and tapered planforms. Results obtained with the modified program are included. Modifications discussed but not incorporated include a state matrix integration method, enhanced vectorization, and use of a cartesian physical mesh.

17. Key Words (Suggested by Author(s))	18. Distribution Statement
Transonic Flow Aeroelasticity Finite Difference Methods Unsteady Aerodynamics	Unclassified--Unlimited Subject Category 02

19. Security Classif. (of this report)	20. Security Classif. (of this page)	21. No. of Pages	22. Price
Unclassified	Unclassified	61	

For sale by the National Technical Information Service, Springfield, Virginia 22161

FURTHER DEVELOPMENT OF XTRAN3S

COMPUTER PROGRAM

C. J. BORLAND
BOEING MILITARY AIRPLANE COMPANY
SEATTLE, WASHINGTON

FINAL REPORT
CONTRACT NAS1-17072

National Aeronautics and
Space Administration
Langley Research Center
Hampton, Virginia

TABLE OF CONTENTS

NOMENCLATURE

a = $\left(\frac{E}{\xi_x}\right) + 2 G_s \xi_y \phi_z$

a = $-\zeta_i \omega_i$ (Section 4.1)

A = $\epsilon_1 M_\infty^2 k^2$

A = state variable coefficient matrix (Section 4.1)

b = $\left(\frac{F}{\xi_x^2}\right) + G_s \xi_y^2$

b = reference span (Section 2.2)

b = $(\omega_i^2 - a^2)^{1/2}$ (Section 4.1)

B = $2 M_\infty^2 k$

B = state variable coefficient matrix (Section 4.1)

c = local section chord nondimensionalized by C_R

C_N = local normal force coefficient

C_m = local pitching moment coefficient

C_x = local axial force coefficient

C_R = reference chord

C_p = local section pressure coefficient

D_ξ, D_η = type-dependent finite difference operators

E = $1 - M_\infty^2$

f = local instantaneous surface section definition

F = $-\frac{1}{2}(\gamma+1)M_\infty^2$

F_z = local normal force

G = $\frac{1}{2}(\gamma-3)M_\infty^2$

G_S = $1 - M_\infty^2$

G_N = $\frac{1}{2}(\gamma-1)M_\infty^2 - 1$

H = $-(\gamma-1)M_\infty^2$

k = nondimensional time scaling

k_c = reduced frequency $\frac{\omega C_R}{U_\infty}$

M = Mach number

M_i = generalized mass of the i^{th} mode

Q_i = total generalized force of the i^{th} mode

q = dynamic pressure

q_i = generalized coordinate of the i^{th} mode

t = time nondimensionalized by $\frac{C_R}{k U_\infty}$

T = physical time

U_n = state variable function

U = freestream velocity

x = streamwise coodinate nondimensionalized by C_R

x_o = local moment reference center

x_{MOM} = global moment reference center

x_n = state variable

X = physical streamwise coordinate

X = function defined by Eq. (13c)

X = state variable matrix (Section 4.1)

y = streamwise coordinate nondimensionalized by C_R

Y = physical streamwise coordinate

Y = function defined by Eq. (13d)

z = streamwise coordinate nondimensionalized by C_R

Z = physical streamwise coordinate

Z_i = generalized force of the i^{th} mode

α = angle of attack

γ = specific heat ratio (1.4 for air)

$\delta_\xi, \delta_\eta, \delta_{\zeta\zeta}$ = finite difference operators

$\Delta\xi, \Delta\eta, \Delta\zeta, \Delta t$ = finite difference numerical step size

ϵ_1, ϵ_2 = $\begin{cases} 0 & \text{low frequency approximation} \\ 1 & \text{otherwise} \end{cases}$

ζ = nondimensional transformed normal coordinate

η = nondimensional transformed spanwise coordinate

Θ = integral of transition matrix (Section 4.1)

Λ_{LE} = leading edge sweep angle

λ = taper ratio

ξ = nondimensional transformed streamwise coordinate

ξ_o = offset of viscous ramp leading edge from some point

ξ_p = length of viscous ramp precursor

ξ_R = length of viscous ramp

ρ = density

ϕ = perturbation velocity potential nondimensionalized by $C_R U_\infty$

Φ = physical velocity potential function, $C_R U_\infty (x + \phi)$

Φ = transition matrix (Section 4.1)

ψ_i = i^{th} vibration mode shape

ω = circular oscillation frequency

Superscripts

$\leftarrow$ = backward difference

$\sim$ = first intermediate solution (prediction)

$\approx$ = second intermediate solution (first correction)

$'$ = spatial derivative

$\cdot$ = time derivative (physical time)

n = previous time level

n+1 = new time level

Subscripts

DN = downstream

i,j,k = ξ, η, ζ grid indices

L = lower surface

LE = leading edge

t	= time derivative (scaled time)
TE	= trailing edge
U	= upper surface
UP	= upstream
$\left\{ \begin{matrix} x,y,z \\ \xi,\eta,\zeta \end{matrix} \right\}$	= spatial derivative
∞	= freestream

FURTHER DEVELOPMENT OF XTRAN3S COMPUTER PROGRAM

FINAL REPORT--CONTRACT NAS1-17072
NASA Langley Research Center
Hampton, Virginia

I. INTRODUCTION

The purpose of this report is to describe further developments and enhancements to the XTRAN3S computer program, a code for calculation of steady and unsteady aerodynamics, and associated aeroelastic solutions, for three-dimensional wings in the transonic flow regime. The program was developed by the Boeing Military Airplane Company (BMAC), Seattle, Washington, under Contract F33615-78-C-3201 to the Flight Dynamics Laboratory of the U.S. Air Force Wright Aeronautical Laboratories, entitled "Transonic Unsteady Aerodynamics for Aeroelastic Applications. The final report on that contract is Refs. 1-3.

Additional work on the program was performed by BMAC under Contract NAS2-10762 to the NASA Ames Research Center, entitled "Addition of Boundary Layer Correction Procedures into Transonic Inviscid Codes (Phase II)". The final report on that contract is Ref. 4.

The present work has been performed under Contract NAS1-17072 to the NASA Langley Research Center. Work reported herein may be summarized by the following list of tasks:

1) The XTRAN3S program, including the boundary layer modifications described in Ref. 4 has been converted to run on the CDC Cyber 203 computer and installed at NASA Langley Research Center;

2) The program has been modified to include a more accurate method of aerodynamic coefficient and generalized force integration than was included in the original version;

3) The input processor of XTRAN3S has been modified to accept surface ordinates and slopes defined at the aerodynamic grid points at the user's option, in addition to the least square error polynomial definition included in the original program;

4) A method of modifying the maximum array dimensions for the aerodynamic and aeroelastic computations has been provided.

5) A modified grid mapping transformation has been included in the program. This will allow accurate and stable computations to be performed for wing planforms with other than very modest degrees of sweep and taper, thus overcoming a major limitation of the original version of the program.

Results of a checkout case for the modified program are included.

In addition, several other potential modifications and improvements, where actual implementation is considered outside the scope of the present effort, are described.

Finally, modifications to the XTRAN3S User's Manual (Ref. 2) and a sample input data set are included as Appendices.

II. XTRAN3S PROGRAM MODIFICATIONS AND ENHANCEMENTS COMPLETED

2.1 Viscous Boundary Layer Modification

The original XTRAN3S program, as described in Refs. 1-3, calculates inviscid transonic flow over three-dimensional wings using a modifed small disturbance finite-difference algorithm. In Ref. 4, the inclusion of a viscous ramp model, used to simulate the displacment effect of a shock-boundary layer interaction, and a two-dimensional quasi-steady strip boundary layer integral method employing the lag entrainment equations due to Green (Ref. 5), was described.

These modifications have now been incorporated in the Version 1.5 of the XTRAN3S code installed on the Cyber 203 at NASA Langley Research Center. In order to exercise the viscous wedge and boundary layer portions of the program, additional input data describing wedge and boundary layer control parameters must be included in the XTRAN3S data input file. These additional data are described in Appendix A.

Test cases have been run on the Langley Research Center Cyber 203 for the inviscid, wedge, and wedge plus boundary layer versions of the code. The test planform was a "typical" transport wing, with a leading edge sweep angle of 30 degrees, a full-span aspect ratio of 8.0 and a taper ratio of 0.4. The airfoil section used was the MBB-A3 8 percent thick airfoil. This case was used as a checkout case for the work described in Ref. 4. Because a modification to the viscous flow portion of the code was made after the results of Ref. 4 were generated, the present report has included some of the recently calculated results. In addition to corrections to the wedge procedure that were not incorporated in Ref. 4., Version 1.5 of XTRAN3S uses a ten-step Runge-Kutta integration of the boundary layer equations, as opposed to the single-step procedure employed in the earlier version. This has been necessary to obtain converged results with the modified grid transformation discussed below. The results are described in a later section of this report. Only steady state results for a rigid wing have been included. The input data for the wedge plus boundary layer test case are given in Appendix B.

2.2 Modified Aerodynamic Coefficient and Generalized Force Integration Method

Aerodynamic coefficients (lift, moment, etc.) have been determined in XTRAN3S by integration of calculated surface pressures, as described in Ref. 1. It has been observed, that since pressures are determined by a process of numerical differentiation, a potential source of error is introduced if the integration and differentiation algorithms are not identical. In steady state calculations, this source of error can be eliminated by calculating section coefficients in terms of circulation, determined by the difference in velocity potential between the upper and lower surfaces at the trailing edge. For unsteady flow, this determination must include other terms and considerations.

In this section, relationships for determining aerodynamic coefficients and generalized forces by an alternate integration method are presented. This alternate representation has been incorporated in the Langley version of XTRAN3S.

For unsteady flow, an approximation to the surface pressure coefficient, consistent with other small disturbance approximations to full potential flow, is given by

$$C_p = -2\phi_x - 2k\phi_t \tag{1}$$

where ϕ is the nondimensional small disturbance potential defined from the full potential

$$\Phi(X,Y,Z,T) = U_\infty C_R [x + \phi(x,y,z,t)] \tag{2}$$

where the physical dimensions X, Y, Z, and T have been nondimensionalized by

$$x = \frac{X}{C_R} \quad ; \quad y = \frac{Y}{C_R} \quad ; \quad z = \frac{Z}{C_R} \quad ; \quad t = \frac{k U_\infty T}{C_R}$$

where C_R is the wing reference chord and k is a nondimensional scaling on time. If k is set to the reduced frequency $\omega C_R / V_\infty$ for a specified oscillatory motion at a circular frequency ω the relation between nondimensional and physical time scales becomes $t = \omega T$.

In the XTRAN3S code, the pressure coefficient Cp was found by a combination of central second-order spatial differencing and first-order backward temporal differencing of the nondimensional disturbance potential expressions of Equation 1.

In solving the dynamic aeroelastic equations of motion for a flexible aircraft structure, the modal approach adopted in XTRAN3S required calculation of the generalized force Q_i

$$Q_i = \iint_S F_z(x,y,t)\, \psi_i(x,y)\, dx\, dy \qquad (3)$$

for the i^{th} elastic mode $\psi_i(x,y)$ where

$$F_z(x,y,t) = \tfrac{1}{2} \rho_\infty U_\infty^2 \left[C_{p_L}(x,y,t) - C_{p_U}(x,y,t) \right] \qquad (4)$$

and L, U denote the lower and upper surfaces.

Numerical differentiation, followed by numerical integration, introduces a truncation error which may be eliminated by application of the following scheme.

Using Equations (1) and (4), we may separate the steady and unsteady parts of the pressure coefficient so that Equation (3) may be written

$$Q_i = 2 q C_R^2 \left[\iint -(\phi_{x_L} - \phi_{x_U}) \psi_i \, dx\, dy \right.$$

$$\left. - \iint k (\phi_{t_L} - \phi_{t_U}) \psi_i \, dx\, dy \right] \tag{5}$$

The first term may now be integrated directly by parts to give

$$Q_i = 2 q C_R^2 \left[\int_{-b/2}^{b/2} -\left[(\phi_L - \phi_U)_{TE} - (\phi_L - \phi_U)_{LE} \right] \psi_i \, dy \right.$$

$$- \int_{-b/2}^{b/2} \int_{LE}^{TE} -(\phi_L - \phi_U) \psi_{x_i} \, dx\, dy$$

$$\left. - \int_{-b/2}^{b/2} \int_{LE}^{TE} k (\phi_{t_L} - \phi_{t_U}) \psi_i \, dx\, dy \right] \tag{6}$$

where the inner integral has been carried out streamwise from the leading to trailing edge of the wing. Note that although the spatial derivative of velocity potential is no longer integrated, the modal slopes ψ_{x_i} are now required as well as modal deflections ψ_i.

For the special cases of normal force, axial force, and pitching moment, the following expressions can be used.

Normal Force: $\psi_i = 1 \quad ; \quad \psi_{x_i} = 0$ (7a)

Axial Force: $\psi_i = f'_{U,L} \quad ; \quad \psi_{x_i} = f''_{U,L}$ (7b)

Pitching Moment: $\psi_i = x - x_{MOM} \; ; \quad \psi_{x_i} = 1$ (7c)

Thus, the sectional force and moment expressions currently written:

$$(cC_N)_j = \int_{LE}^{TE} (C_{p_L} - C_{p_U})\, dx \tag{8a}$$

$$(c^2 C_m)_j = -\int_{LE}^{TE} (C_{p_L} - C_{p_U})(x - x_o)\, dx \tag{8b}$$

$$(cC_x)_j = -\int_{LE}^{TE} (C_{p_L} f'_L - C_{p_U} f'_U)\, dx \tag{8c}$$

may be rewritten as follows:

$$(cC_N)_j = -2(\phi_{TE_L} - \phi_{TE_U}) - 2k \int_{LE}^{TE} (\phi_{t_L} - \phi_{t_U})\, dx \tag{9a}$$

$$(c^2 C_m)_j = -\left\{ -2\left[(x_{TE} - x_o)(\phi_{TE_L} - \phi_{TE_U}) - \int_{LE}^{TE} (\phi_L - \phi_U)\, dx \right] - 2k \int_{LE}^{TE} (\phi_{t_L} - \phi_{t_U})(x - x_o)\, dx \right\} \tag{9b}$$

$$(CC_x)_j = -\left\{-2\left[\left(\phi_{TE_L} f'_{TE_L} - \phi_{TE_U} f'_{TE_U}\right) - \left(\phi_{LE_L} f'_{LE_L} - \phi_{LE_U} f'_{LE_U}\right)\right.\right.$$

$$\left.\left. - \int_{LE}^{TE} \left(\phi_L f''_L - \phi_U f''_U\right) dx\right] - 2k \int_{LE}^{TE} \left(\phi_{t_L} f'_L - \phi_{t_U} f'_U\right) dx\right\} \quad (9c)$$

Note that for the axial force term: 1) the leading edge terms do not cancel out as with the generalized force or lift and moment expressions, due to the difference in slope on the upper and lower surface, and 2) the surface curvature f" must be available as well as the slope. The curvature is calculated internally by differencing the slopes. The remaining integrals are carried out by the Simpson's Rule method as before. These alternate formulations for normal force pitching moment, axial force, and generalized force, have been incorporated in the present version of XTRAN3S.

2.3 Direct Input of Surface Ordinates and Slopes

In the original version of the XTRAN3S program, airfoil section geometry was defined in terms of separate polynomials describing the upper and lower surface. The coefficients and exponents of the surface polynomial were usually to be obtained from a least-squares error curve fitting procedure. This is the "FUNCTIONAL" option for airfoil geomtry input defined in Ref. 2.

In order to allow the user to input a surface geometry definition obtained from any alternate method (such as a cubic spline fit) an alternate input method has been included, defined as the "TABULAR" option. The exact form of the required input data is described in Appendix A. When the TABULAR option is exercised for a given airfoil section, the program expects nondimensional input data in the form of streamwise distance in percent of local chord and upper or lower surface ordinates and streamwise slopes at the aerodynamic mesh points ("XI MESH") which will be used in the finite difference solution. Note

that the input and computational points must correspond exactly as no interpolation is performed in the streamwise direction. A sample data set including the "TABULAR" data option is given in Appendix B.

2.4 Variable Array Dimensions

The size of computational arrays for XTRAN3S were originally determined by the limitations of core storage of the CDC 7600 computer. The computational mesh was used for 60 streamwise, 20 spanwise, and 40 vertical mesh points, including the outer mesh boundaries. The effect of varying these numbers of points on the accuracy or stability of the solutions has not been assessed.

Because of the virtual memory features of the Cyber 203 system an absolute core limitation is no longer applicable. A method for using alternate sizes of flow field computational arrays, as well as surface boundary conditions and number of mode shapes, has been provided. Because the current version of Cyber 203 Fortran does not support PARAMETER-type data specification, it is necessary for the user to modify a file containing several UPDATE correction sets. These correction sets are then used to create a modified source program, which is then compiled and run in the usual fashion. The UPDATE correction sets that have been included in the current Cyber 203 version are stored on files at the NASA Langley computing facility. The files containing these correction sets may be modified by using a change option in a standard text editor, such as XEDIT. Note that in allocation statements (DIMENSION, REAL, etc.) actual values must be substituted for the variable names defined below. In DATA statements, actual numerical values are changed as required. Statements which define the limits of DO loops or dimensions passed through calling sequences may be changed at the user's option. The following parameters and their default values are defined in the correction sets and may be changed by the user:

Parameter	Definition	Default Value
DNXIW	Maximum number of streamwise grid points on the wing surface	50
DNETAW	Maximum number of spanwise grid points on the wing surface	20

DNXIT	Maximum number of total streamwise grid points	60
DNETAT	Maximum number of total spanwise grid points	20
DNZT	Maximum number of total vertical grid points	40
DNMAES	Maximum number of total generalized aeroelastic coordinates	20
DNSAES	Maximum number of structural degrees of freedom for aeroelastic solutions inertia force points	100
DNFAES	Maximum number of external force degrees of freedom for aeroelastic solutions	20
DNMODES	Maximum number of specified modal motions	5

Note that any or all of these parameters may be changed separately by the procedure. Since the correction sets are incorporated in the modified old program library with the default dimensions, it will be necessary to YANK these existing sets, modify them, and replace it during the UPDATE procedure. (Familiarity with the terminology of the CDC UPDATE system is assumed here. Other readers may consult the UPDATE Reference Manual, Ref. 6.)

2.5 Modified Grid Mapping Transformation

Various studies with XTRAN3S, by investigators at BMAC and several other aerospace companies, NASA Ames, NASA Langley, and the Air Force have shown that, while the program could perform adequately for moderate-to-high aspect ratio wings, it was difficult or impossible to obtain converged solutions for low or high aspect ratio wings with more than moderate degrees of sweep and taper. These numerical difficulties were found to be primarily a consequence of the grid transformation system employed in the XTRAN3S numerical algorithm. This grid transformation tended to give a highly skewed physical mesh in the wing plane with distortion of the outer mesh boundaries, as shown schematically in Fig. 1. A modified grid mapping scheme results in a grid with rectangular outer boundaries in both the physical and computational spaces illustrated in Fig. 2. This mesh has a reduced degree of skewness in regions away from the wing and has apparently alleviated these numerical difficulties.

In the current method, separate grid stretching schemes are applied in the regions ahead of, over, and behind the wing. As the transformations are linear within the three regions, no attempt has been made to retain second derivative continuity at the wing boundaries. This does not seem to signficantly affect the results described below, however.

In the original version of XTRAN3S, the following shearing transformation was applied in order to map a swept tapered planform in the physical domain into a rectangular wing planform in the Cartesian computational domain:

$$\xi = \frac{x - x_{LE}(y)}{c(y)} \; ; \; \eta = y \; ; \; \zeta = z \qquad (10a)$$

In the modified scheme, the following transformation is applied for points ahead of the wing leading edge ($x < x_{LE}$)

$$\xi = (x - x_{LE}(y))\left(\frac{x_{UP}}{x_{UP} - x_{LE(y)}}\right) \qquad (10b)$$

For points downstream of the trailing edge ($x > x_{TE}$) the following transformation is applied:

$$\xi = (x - x_{TE}(y))\left(\frac{x_{DN} - 1}{x_{DN} - x_{TE}(y)}\right) + 1 \qquad (10c)$$

where x_{UP} and x_{DN} define the upstream and downstream limits, respectively, of both the physical and computational meshes, nondimensionalized with respect to C_R. In the region over the wing, Equation (10a) defines the mesh transformation as before. It may easily be seen that at the following limits, these limiting values of the transformation are obtained:

$$\text{at } x = x_{UP} \qquad \xi = x_{UP} \tag{11a}$$

$$\text{at } x = x_{LE}(y) \qquad \xi = 0 \tag{11b}$$

$$\text{at } x = x_{TE}(y) \qquad \xi = 1 \tag{11c}$$

$$\text{at } x = x_{DN} \qquad \xi = x_{DN} \tag{11d}$$

In the current scheme, the linear stretching in the three different regions yields a discontinuity in the second derivative of the mesh spacing. Although other transformation schemes are possible and could be easily incorporated, the present approach has shown considerable improvement in convergence of the results when compared with the previous version of XTRAN3S.

Since the coordinate transformation employed enters directly into the numerical algorithm employed in XTRAN3S, the final expression of the ADI numerical scheme, Eq. 21 of Ref. 1, must now be re-written as follows:

i) ξ-sweep:

$$B\,\bar{\delta}_\xi\left(\frac{\tilde{\phi}-\phi^n}{\Delta t}\right) = D_\xi\left[a^n\left(\frac{\tilde{\phi}_\xi-\phi_\xi^n}{2}\right)+c\,\phi_\xi^n\,\tilde{\phi}_\xi\right]$$
$$+2G_s\left(\delta_\eta\,\phi^n\right)D_\eta\left(\bar{\delta}_\xi\,\phi^n\right)+\delta_\eta\left(\frac{1}{\xi_x}\,\delta_\eta\,\phi^n\right)$$
$$+\delta_\xi\left(\frac{1}{\xi_x}\,\delta_\xi\,\phi^n\right)+\delta_\xi X^n+\delta_\eta Y^n \tag{12a}$$

ii) η-sweep:

$$B\,\overleftarrow{\delta}_\xi\left(\frac{\tilde{\tilde{\phi}}-\tilde{\phi}}{\Delta t}\right)=\frac{1}{2}\delta_\eta\left(\frac{1}{\xi_x}\delta_\eta\,\tilde{\tilde{\phi}}-\frac{1}{\xi_x}\delta_\eta\,\phi^n\right)$$

$$+G_s\left(\delta_\eta\,\phi^n\right)D_\eta\left(\overleftarrow{\delta}_\xi\,\tilde{\tilde{\phi}}-\overleftarrow{\delta}_\xi\,\phi^n\right) \qquad (12b)$$

iii) ζ-sweep:

$$\frac{A}{\xi_x}\left(\frac{\phi^{n+1}-2\phi^n+\phi^{n-1}}{\Delta t^2}\right)+B\,\overleftarrow{\delta}_\xi\left(\frac{\phi^{n+1}-\tilde{\tilde{\phi}}}{\Delta t}\right)=$$

$$\frac{1}{2}\delta_y\;\;\frac{1}{\xi_x}\delta_y\left(\phi^{n+1}-\phi^n\right)\Big] \qquad (12c)$$

where the forms of the coefficients and difference operators are as defined in Ref. 1, except that:

$$a=\xi_x\left[E+2G_s\left(\frac{\xi_y}{\xi_x}\right)\phi_\eta\right] \qquad (13a)$$

$$b=\xi_x^2\left[F+G_s\left(\frac{\xi_y}{\xi_x}\right)^2\right] \qquad (13b)$$

$$X=\xi_y^2\left(G_N+H\right)\phi_\xi^2+\xi_y\left(2G_N+H\right)\phi_\xi\,\phi_\eta$$

$$+\left[G_N\,\phi_\eta+\left(\frac{\xi_y}{\xi_x}\right)\xi_y\right]\phi_\eta+\left(\frac{\xi_y}{\xi_x}\right)\xi_y\,\phi_\xi \qquad (13c)$$

and

$$Y = \frac{\xi_x}{\xi_y}\phi_\xi + H\xi_y\phi_\xi^2 + H\phi_\xi\phi_\eta \qquad (13d)$$

The following forms of the transformation derivatives have been used:

For $x < x_{LE}$:

$$\xi_x = \frac{\chi_{UP}}{\chi_{UP} - \chi_{LE}(y)} \quad ; \quad \xi_y = \frac{\chi_{UP}\cdot\chi'_{LE}(y)(\chi - \chi_{UP})}{(\chi_{UP} - \chi_{LE}(y))^2} \qquad (14a)$$

for $x_{LE} \leq x \leq x_{TE}$;

$$\xi_x = \frac{1}{C(y)} \quad ; \quad \xi_y = \frac{-(\chi'_{LE}(y) - \xi C'(y))}{C(y)} \qquad (14b)$$

For $x > x_{TE}$:

$$\xi_x = \frac{\chi_{DN} - 1}{\chi_{DN} - \chi_{TE}} \quad ; \quad \xi_y = \frac{(\chi_{DN}-1)(\chi'_{TE}(y))(\chi - \chi_{DN})}{(\chi_{DN} - \chi_{TE}(y))^2} \qquad (14c)$$

III. RESULTS FOR MODIFIED COMPUTER PROGRAM

A modified version of a computer program XTRAN3S is available for calculating the steady and unsteady aerodynamic loads and aeroelastic response of thin clean wings in transonic flow. All of the results presented here were generated using Version 1.5 of XTRAN3S on the NASA Langley Cyber 203 system. The basic code has been modified to account for viscous effects by incorporating the method of Ref. 4, and other modifications described above. Appendix A describes alterations in user input specifications for the modifed version of XTRAN3S.

For the sample case considered, calculations were performed which generated an inviscid solution, a solution using the viscous ramp alone, and a full viscous solution employing the viscous ramp in conjunction with the boundary-layer equations.

All computations were performed on a nonuniform 60 x 20 x 40 (ξ, η, ζ) Cartesian computational mesh with the wing surface defined by 39 x 12 points in the ξ - η plane. The computational domain was defined by

$$-15.375 \leq \xi \leq 26.575$$

$$0 \leq \eta \leq 5.3$$

$$-13.0375 \leq \zeta \leq 13.0375$$

and minimum grid spacing taken as

$$\Delta\xi_{min} = 0.01$$

$$\Delta\eta_{min} = 0.10$$

$$\Delta\zeta_{min} = 0.025$$

which occur at the wing leading edge, at the wing tip, and adjacent to the wing surface respectively. XTRAN3S default values were employed for the ξ- and ζ-mesh distributions. The η-mesh and surface geometry description for the case considered may be found in Appendix B. For all calculations the time scaling, k, was selected as 0.2 and a time step of $\Delta t = 0.0034906585$ was employed. This corresponds to a distance of one root chord of travel in 57.3 time steps at the freestream velocity. For a reduced frequency of $k_c = 0.2$, the choice of Δt results in five time steps per degree of circular frequency change along the pitching cycle of a forced oscillation. Nominal values of the viscous ramp parameters were selected as follows:

$$\xi_o = 0.02,$$
$$\xi_p = 0.02,$$
$$\xi_R = 0.10.$$

These choices have proven adequate for a number of both steady and unsteady two-dimensional solutions. Results were generated on the Cyber 203 computing system and required approximately 2.1 seconds of CPU time per time step of calculation for both inviscid and wedge alone solutions, and 3.8 seconds per time step for full viscous computations. No attempt has been made to optimize the executable code for the Cyber 203.

All converged steady state solutions were run for 900 time steps at the indicated values of k and Δt. These choices were found to be conservative with respect to both stability and convergence. The low frequency approximation (i.e., $\epsilon_2 = 0$) was made in the wake jump condition (Eq. 10a of Ref. 4) and downstream boundary condition (Eq. of Ref. 4). In general, the following procedure was employed in generating steady-state results:

i) a converged inviscid solution was obtained using an undisturbed condition as an initial state (i.e., $\phi = \phi_t = 0$);

ii) a converged wedge alone solution was obtained using the inviscid solution as the initial state, updating the wedge computation at each time step;

iii) a converged full viscous solution was obtained using the wedge alone solution as the intial state, updating the boundary-layer computation at each time step.

For the sample case, a typical transport wing planform and a section geometry corresponding to the MBB-A3 airfoil were chosen. A wing planform identical to the Lockheed-Georgia "Wing A" was employed (AR = 8.0, λ = 0.4) except that the leading edge sweep angle was set to 30^{0}. The planform is shown in Fig. 3a. The airfoil section, shown in Fig. 3b, has a blunt leading edge, a thickness ratio of 8.9 percent, moderate aft camber, and has been selected as an AGARD standard for evaluating transonic aeroelastic analysis methods.

Steady-state solutions were generated for inviscid, wedge alone, and fully viscous cases for freestream conditions corresponding to M_{∞} = 0.85, α = 1.0^{0} and $Re_{\infty} = 10^{7}$. Results of the pressure distributions at four spanwise mesh stations are compared in Fig. 4. Viscous effects near shocks and on the aft lower surface are apparent. It is recommended that the wedge-alone procedure not be used except as an intermediate step, as this gives only a partial compensation for viscous flow effects, and yields physically unrealistic answers.

IV. ADDITIONAL POTENTIAL MODIFICATIONS AND ENHANCEMENTS TO THE XTRAN3S COMPUTER PROGRAM

4.1 State Transition Matrix Structural Integrator

The dynamic equations of motion for an elastic airplane may be formulated in terms of generalized displacement response q_i which are solutions of the following set of equations:

$$M_i \ddot{q}_i + M_i [2\zeta_i \omega_i] \dot{q}_i + M_i \omega_i^2 q_i = Z_i \; ; \; i = 1, 2, 3, \ldots N$$

where

$$M_i = \iint_S \psi_i^2(x,y)\, \rho(x,y)\, dS \qquad \text{generalized mass}$$

and

$$Z_i = \iint_S F_z(x,y,t)\, \psi_i(x,y)\, dS \qquad \text{generalized force}$$

of the i^{th} generalized coordinate $\psi_i(x,y)$ (usually representing vibration modes of natural frequency ω_i), and ζ_i are the assumed modal damping factors.

In Ref. 7, the dynamic problem was formulated (for a two-dimensional case) in terms of a state variable equation of the form

$$\dot{x} = A x + B u$$

and a state transition matrix integrator

$$x_{n+1} = \Phi x_n + \frac{1}{2} \Theta B (3 u_n - u_{n-1})$$

was employed. This form of numerical integration can be used if the problem is re-formulated in the following manner:

In general, the dynamic problem can be written as a matrix equation

$$\{\ddot{q}_b\} + [M]^{-1}[G]\{\dot{q}_b\} + [M]^{-1}[K]\{q_b\} = [M]^{-1}\{F(t)\}$$

where [M], [G], and [K], are the generalized mass, damping, and stiffness matrices, respectively, and $\{F(t)\}$ is the time-varying generalized force, including aerodynamic and external force contributions, if any.

The problem may now be recast in state variable format by letting

$$X = \begin{Bmatrix} q_b \\ \dot{q}_b \end{Bmatrix} \qquad (2N \times 1)$$

then

$$\dot{X} = AX + Bu$$

where

$$A = \begin{bmatrix} 0 & I \\ -[M]^{-1}[K] & -[M]^{-1}[G] \end{bmatrix} \qquad (2N \times 2N)$$

$$B = \begin{bmatrix} 0 \\ [M]^{-1} \end{bmatrix} \qquad (2N \times N)$$

$$u = \{F(t)\} \qquad (N \times 1)$$

Two cases can be considered: a) where the generalized coordinates represent orthogonal modes, and b) where the generalized coordinates are non-orthogonal or where additional matrix elements, such as control system coupling terms, have been added.

In case a) the generalized mass, stiffness, and damping matrices are diagonal, and analytical forms of the integration matrices Φ and Θ exist. Reorganizing the state vector such that the states for each normal mode are grouped together, $x^T = (q_1, \dot{q}_1, q_2, \dot{q}_2, \ldots, q_N, \dot{q}_N)$ yields a system A matrix with diagonal (2x2) submatrices composed fropm the frequency, ω_i, and damping ζ_i of the i^{th} mode. For each degree of freedom, the (2x2) matrix of elements of the state transition matrix Φ are defined as

$$\Phi = e^{At} = \begin{bmatrix} \left(e^{at}\cos bt - \frac{a}{b}\sin bt\right) & \left(\frac{1}{b}e^{at}\sin bt\right) \\ \left(-\frac{(a^2+b^2)}{b}e^{at}\sin bt\right) & \left(e^{at}\cos bt + \frac{a}{b}e^{at}\sin bt\right) \end{bmatrix}$$

and the elements of the integral of the transition matrix Θ are

$$\Theta_{11} = \frac{e^{at}}{a^2+b^2}\left[-2a\cos bt + \left(b - \frac{a^2}{b}\right)\sin bt\right]$$

$$\Theta_{12} = \frac{e^{at}}{a^2+b^2}\left[\frac{a}{b}\sin bt - \cos bt\right]$$

$$\Theta_{21} = \frac{-e^{at}}{b}\left[a\sin bt - b\cos bt\right]$$

$$\Theta_{22} = \frac{e^{at}}{a^2+b^2}\left[\left(b + \frac{a^2}{b}\right)\sin bt\right]$$

where for each individual normal mode

$$a = -\zeta_i\omega_i \qquad b = \left(\omega_i^2 - a^2\right)^{1/2}$$

and hence

$$\zeta_i = -\frac{a}{a^2+b^2}$$

and t is the integration step size.

For case b), analytical forms of the transition matrix are not available, and a partial series approximation of the form

$$\Phi = e^{At} = I + At + \frac{1}{2!}A^2t^2 + \frac{1}{3!}A^3t^3 + \cdots + \frac{1}{n!}A^nt^n$$

$$\Theta = \int_0^t e^{A(t-\tau)}d\tau = It + \frac{1}{2!}At^2 + \frac{1}{3!}A^2t^3 + \cdots + \frac{1}{n!}A^{n-1}t^n$$

may be employed.

It may be noted that since the elements of the Φ and θ matrices are dependent only on the values of ω_i and ζ_i for case a), or on the input matrices [M], [G], and [K] they need be calculated only once.

Implementation of the transition matrix scheme may be accomplished in XTRAN3S by modifying (or providing a special version) of the subroutine AEROEL, since all structual integration is accomplished within that routine. The input natural free vibration frequencies ω_i and the damping coefficients ζ_i may be determined externally and input directly (this requires modification of the input processor) or determined from the input mass generalized, damping and stiffness matrices by the following relationships:

$$\left[\omega_i^2\right] = \left[M\right]^{-1}\left[K\right]$$

$$\left[\zeta_i\right] = \frac{1}{2}\left[K\right]^{-\frac{1}{2}}\left[M\right]^{-\frac{1}{2}}\left[G\right]$$

An UPDATE correction set for incorporating the state transition matrix integration procedure is stored on file at the NASA Langley computing facility. This may be incorporated directly into the modified version of the program or modified as desired. No aeroelastic check cases have been run using this new procedure, as this was considered outside the scope of the present effort.

4.2 Efficiency Improvement Through Enhanced Vectorization*

The original version of XTRAN3S was developed using the CDC 7600 computer. During the code development period, advanced vector machines, such as the Cyber 203 and CRAY-1S, became available. The code was adapted to operate on these two machines, but only minimal changes to the code were performed to take advantage of "implicit" vectorization, i.e., those portions of the code that could easily be adapted to vector computation through the existing nature of the computational algorithm described in Ref. 1.

Later studies with a pilot code version of XTRAN3S, operational on the CRAY-1S, showed that at least a factor of two improvement in computational efficiency could be achieved by rearrangement of operations to permit a larger degree of implicit (or automatic) vectorization. (This represents a speed-up factor of almost five compared to an unvectorized or scalar code operating on the same machine.) These concepts are generally applicable, but not directly transportable, to the Cyber 203 version of the code, since the Cyber 203 requires longer vectors than the CRAY-1S to achieve improved efficiency when compared with scalar computations.

In this section, the original algorithm of Ref. 1 will be described with respect to its implications for vectorization. Then the modifications necessary to achieve a higher degree of vectorization on the CRAY-1S will be discussed, and finally the adaptation of those modifications to the Cyber 203 will be discussed.

As shown in Equation (12) above, the computational algorithm for solution of unsteady transonic flow implemented in XTRAN3S is an alternating-direction implicit (ADI) scheme employing approximate factorization to solve the modified transonic small disturbance potential equation, via a finite difference approximation. The original partial differential equation has been replaced by a set of algebraic equations for potential at a finite number of grid points. Starting from a known or given value of the potential φ^n at a given time t^n, the solution is advanced to $t^{n+1} = t^n + \Delta t$ via a

*NOTE: The reader is assumed to be familiar with the concepts of vectorization employed by "pipeline" computers such as the CRAY-1S and Cyber 203.

series of "predictor-corrector" steps. Equation 12 represents three sets of matrix equations, with the solution or "sweep" direction corresponding to a coordinate of the computational mesh. Each equation is solved implicitly for the value of the potential along the sweep direction. The number of equations so solved is the product of the number of points in the computational mesh in the other two cordinates. Thus, if the number of points in the computational mesh in the ξ, η, and ζ directions are N_ξ, N_η, and N_ζ respectively, the following represents the number of solutions required to advance the potential solution one step:

ξ-sweep: $N_\eta \times N_\zeta$ equations, length N_ζ

η-sweep: $N_\zeta \times N_\xi$ equations, length N_η

ζ-sweep: $N_\zeta \times N_\eta$ equations, length N_ζ

For the η and ζ sweeps, the equations are tridiagonal, i.e., a matrix formulation has non-zero terms only on the diagonal elements and in elements adjoining the diagonal. The ξ sweep equations are lower quadra-diagonal due to the use of a mixed difference operator, i.e., backward differences in regions of supersonic flow and central differences in regions of subsonic flow, with a combined shock-point operator.

The solution process for each equation set (sweep) involves four distinct steps: a) formulation of the left-hand side, b) formulation of the right-hand side, c) solution, and d) setting of field and boundary condition values of potential based on this solution.

Since formulation of the left- and right-hand sides are essentially repetitive statements of the finite difference approximations, as are the boundary conditions, these portions are particularly well adapted to vectorization. The solution process, on the other hand, employs a recursive algorithm and thus cannot be directly vectorized. Several alternate formulations of the solution process including vectorizable solution algorithms, were evaluated, but proved to provide less improvement in efficiency than the method described below.

In the original version of XTRAN3S, the equations for the ξ-sweep, Equation (12a) are solved sequentially for each η mesh point, with a constant ζ mesh point location. Thus for the default values of $N_\xi = 60$, $N_\eta = 20$, $N_\zeta = 40$, 20 equations of length 60 are solved for each ξ-η plane. Then, for the same ξ-η plane, the η-sweep equations (60 equations of length 20) are solved sequentially in the downstream (increasing ξ) direction due to the presence of the backward spatial or "upwind" difference approximation to ϕ_{xt}. This process is then repeated for the next ξ-η plane in the increasing ζ direction. The ζ-sweep is performed by accessing the data, formulating the equations, and solving for each ξ-ζ plane sequentially in the increasing downstream direction, with the process then repeated for the next plane in the increasing η direction. Since solutions of the ζ-sweep equations, φ^{n+1}, are dependent on φ^n, φ^{n-1} and the solution of the η-sweep equations $\tilde{\tilde{\varphi}}$, but not on the solutions to the ξ-sweep equations, $\tilde{\varphi}$ need not be stored in a three-dimensional array.

The process of the three sweeps for the original scheme and the access of the data from the three-dimensional to two-dimensional arrays, are illustrated in Figure 5.

With the availability of the CRAY 1S and Cyber 203, with features of vectorization and very large available storage, other data arrangement and sweeping schemes have been investigated. In addition, a method for vectorization of the tridiagonal and quadradiagonal solution algorithms has been employed. This method, suggested by the work of J. Lambiotte of NASA Langley Research Center, formulates each step of the tridiagonal or quadradiagonal recursive solution procedure as a vector operation (or vectorizable do-loop). Since for the η and ζ sweeps the equations are inter-dependent in the ξ direction, reorganization of solutions is required for vectorization.

For the CRAY-1S, the scheme illustrated by Figure 6 has been adopted. For the ξ-sweep, data is accessed mutually for each ξ-ζ plane (rather than each ξ-η plane), and a vectorized solution is performed in the ζ direction, i.e., each step in the solution process is a vector operation of length 40.

This is then repeated for the next ξ-ζ plane, and the intermediate result $\tilde{\varphi}$ is stored in a three-dimensional array. For the η-sweeps, the data is accessed in the η - ζ planes, and a vectorized solution of length 40 is again performed in the ζ direction, with the results $\tilde{\tilde{\varphi}}$ stored in a three-dimensional array. Finally, the ζ-sweeps are performed as a vectorized solution of length 20 in the η direction, and the advanced values of the potential φ^{n+1} are stored in place of the values φ^n at the previous time step. It should be noted that four three-dimensional "levels" of storage, φ^n, φ^{n-1}, $\tilde{\varphi}$, and $\tilde{\tilde{\varphi}}$ are required for this scheme, compared with three for the original scheme. In addition, however, nine additional three-dimensional arrays for vector equation coefficients and right-hand sides have been stored to improve efficiency and decrease the amount of re-calculation required. For the default mesh, the amount of storage for three-dimensional arrays has increased from 144,000 to 624,000. The total storage requirement has thus increased from about one-half million words to over one million words.

Since efficiency on the Cyber-203 is improved with very long vectors, the following modification to the above scheme is recommended. For the ξ-sweep, each ξ-ζ plane is treated separately although each of the 800 (=20x40) ξ-sweep equations is independent. It should prove possible to reorganize the ξ-sweep equation solution into a single vector operation of length 800. The η and ζ sweeps, however, would still require sequential vector operations of length 40 and 20 due to upstream dependence. If the improved efficiency of 800 length vector operation is realized, a significant speedup could be accomplished as a comparatively large portion (45 percent) of the computational workload occurs in the ξ-sweep due to the large number of operations performed.

An alternate approach would be the use of a vectorized solution algorithm such as cyclic reduction as discussed by Lambiotte (Ref. 8), Calahan, et al (Ref. 9), and others. The method would involve considerable rearrangement of the data into very long vectors. The 800 ξ-sweep equations could be solved as a single vector of length 48,000 provided the data is arranged in matrix

form so that the equations are properly decoupled. The η-sweep and ζ-sweep equations could be rearranged with each η-ζ plane into vector operations of length 800. Experience with these methods has been less than encouraging, however, and the improved scalar efficiency of the Cyber 203 as compared to the STAR-100 may make this approach undesirable.

4.3 Efficiency Improvement by use of a Cartesian Physical Mesh

As described in Section 2.5 above, the original version of XTRAN3S has been modified to incorporate different physical to computational mesh transformations in various regions of the flow field, provide a mesh with reduced skewness, as illustrated in Figure 2. Computations with the scheme on lower aspect ratio, highly tapered wings has shown that computational reliability has significantly improved, i.e., solutions that were previously unstable could now be obtained. Computational efficiency, as measured by the size of the time step required, and thus the amount of CP time, to obtain a converged steady or unsteady solution was not apparently improved. This is a reasonable finding, since the basic stability of the algorithm is controlled by the explicit treatment of the cross-terms (e.g. $\phi_{\xi\eta}$) in the transformed modified small disturbance equation.

An alternate approach, considered early in the program development but rejected, would be the use of an identical physical and computational fully Cartesian mesh and solution of the original (untransformed) modified small disturbance potential equation on this mesh. This scheme was rejected because of a) the increased amount of data manipulation required for a mesh not aligned with planform edges, b) the occurrence of misalignment between physical and computational boundary condition points, possibly causing severe pressure fluctuation as observed in Mach-box schemes, and c) the apparent success of the mesh transformation scheme of Equation (10a), as illustrated by the Bailey-Ballhaus method for steady three-dimensional transonic flow.

It has been postulated that computational stability, and thus efficiency, could be improved if explicit treatment of the cross terms could be avoided. Use of a fully implicit algorithm on the transformed mesh showed no

significant improvements, for reasons not understood at this time. However, modifications of the pilot code to incorporate a fully Cartesian mesh has been performed with the result of a significant improvement in the size of the time step allowed.

Figure 7 illustrates schematically the Cartesian physical and computational mesh used for the F-5 wing model, compared with Figure 1 and 2, which use the transformed grid with distorted and rectangular outer boundaries, respectively. With a time scaling variable, k, of 1.0, a time step of approximately .0145 was required to obtain a converged rigid steady solution for the F-5 wing at $.5^{0}$ angle of attack and a Mach number of .95 using the transformed grid. With the Cartesian grid, this maximum time step could be increased to approximately .0872 improving computational efficiency by a factor of 6.

This improvement in stability is apparently due to the removal of several of the cross terms from the equation, and the reduction in magnitude of others due to removal of the transformation scaling factors ξ_x and ξ_y.

There are two potential disadvantages, however, and the user must consider these in the context of his particular problem:

a) The grid must be tailored to each individual planform by aligning mesh points at a uniform spacing with respect to the leading edge (1/2 percent behind the leading edge, for example), to avoid spanwise pressure fluctuations (this has shown to be less critical with respect to the trailing edge, but this must be considered as well); for a constant swept leading edge, uniform grid spacing in both chordwise and spanwise directions is thus required.

b) There will be some loss of resolution in the pressure distributions, and hence possible inaccuracies in intergrated aerodynamic coefficients and generalized forces, especially near the tips of highly tapered planforms. On the F-5 wing, for example, a grid of 45 mesh points on the wing root chord yield only 13 points at the tip chord. This loss of

resolution is also seen in the details of pressure distributions near the leading edge. It may be necessary to enforce minor modifications to leading edge slopes to achieve the right degree of expansion around the leading edge. Here, other available solutions such as experimental data, full potential, or XTRAN3S with the transformed grid system, may provide guidance.

Comparison of calculated pressures with the viscous boundary-layer approximation for the F-5 wing using the transformed and Cartesian grids are shown in Figs. 8 and 9. Also shown are the experimental data of Ref. 10. It may be seen that overall pressure levels are adequately predicted, but shock locations are expecially near the tip, somewhat further aft for the Cartesian grid. This is typical of numerical methods with increased dissipation due to the truncation errors of the coarser mesh. No evaluation of this new approach has been performed for unsteady or aeroelastic solutions at the present time.

With the modifications described in Section 4.2 and 4.3 incorporated in the pilot code, a converged solution for the rigid F-5 wing at a constant angle of attack can be obtained in about 90 seconds of CP time on the CRAY-1S. It is estimated that unsteady aeroelastic solutions, such as described in Ref.11, could be obtained in about 3 minutes CP time for each Mach number, dynamic pressure combination. These estimates would vary for the Cyber 203, depending on the degree of vectorization that could be applied and the speedup achieved.

V. CONCLUSIONS

The XTRAN3S computer program, for calculation of unsteady transonic flow and aeroelastic solutions for three-dimensional thin clean wings, has been modified and enhanced, and these improvements have been incorporated in Version 1.5 installed on the Cyber 203 system at NASA Langley Research Center.

These modifications and enhancements consist of:

1) Incorporation of a viscous boundary layer method;

2) Incorporation of a modified integration method for aerodynamic coefficients and generalized forces;

3) Modification of the input processor to accept direct input of surface ordinates and slopes, as well as least-square polynomial coefficients;

4) A method of modifying the maximum array dimensions for aerodynamic and aeroelastic computations; and

5) A modified grid transformation to provide reduced skewness for the physical mesh, improving the ability of the code to obtain solutions for swept, tapered planforms.

Other potential modifications have been presented and discussed, including:

1) Incorporation of a state transition matrix method for structral integration in aeroelastic problems;

2) Efficiency improvement through enhanced vectorization; and

3) Efficiency improvement through incorporation of a Cartesian physical mesh.

Results of computation on the Cyber 203 using the modified version of the program have been presented.

Modifications to the User's Manual for XTRAN3S and a sample data set have been incorporated Appendices.

APPENDIX A

MODIFICATION OF XTRAN3S INPUT DATA REQUIREMENTS

The input data required by XTRAN3S is in the form of a card deck or a card image file. All data is free field. Section A describes the input data deck structure while Section B spells out the required input cards for implementation of the direct input and viscous options and the associated formats and ground rules. This Appendix may be considered as a revision of Section V of Ref. 2, and should be used in conjunction with that Section.

A. Input Data Deck Structure

The input data deck for XTRAN3S has four levels of organization.

1. Program Deck - This includes all inputs for one problem. The deck "boundaries" are

   first record - BEGIN PROBLEM DEFINITION

   last record - END OF PROBLEM

2. Data Section - A program deck is divided into data sections. Specifically, the deck is divided into the following ten data sections:

   1) Problem Definition Section
   2) Computational Control Section
   3) Computational Grid Section
   4) Geometry Section
   5) Boundary Condition Section
   6) Structural Modal Section
   7) Structural Matrix Section
   8) Checkpoint/Restart Section
   9) Post-processing Section
   10) Viscous Calculation Section

As noted previously, the first section must be the Problem Definition Section. The order of the remaining sections is immaterial. The first record in each section must be of the form "BEGIN etc." No section terminator is required.

3. Data Record - Sections are in turn divided into data records or statements. As noted above, the first record is of the form "BEGIN etc." In most cases the order of the remaining records in the section is immaterial. All exceptions to this rule are specifically noted. Record boundaries are governed by the following rules.

   - o If the last non-blank character on the card is a "+" then the record continues onto the next card.
   - o Maximum record length is 250 items.
   - o Record terminators are / or card boundaries.
   - o The space between / and the card boundary is "ignored" and hence is available for comments. If a record is only comment it must begin with */.

4. Data Item - Records are in turn composed of data items. This is the finest level of subdivision for the program deck. The delimiters or "boundaries" of items are of two types.

   - o colon : this is used at most once per record and then only after keywords.
   - o commas, blank spaces and record terminators.

B. Record Formats

The following ground rules concerning notation apply throughout this section.

a) [[ ]]-- Data items enclosed by double brackets have optional input formats. One or more of the indicated options must be selected.

b) [ ]-- Data items enclosed by brackets have optional input formats. Only one of the indicated options must be selected.

c) ( )-- Data items enclosed by parentheses have default values. If the default is acceptable for definition of the problem data, the particular item or items need not be input. All default values are defined in the descriptions of the input data.

d) ITEM -- An item typed in all upper case letters is called a key-word. At least the underlined portion of a key-word must be input. This is always the first four characters including trailing blanks.

e) Item -- An item with only the leading character typed in upper case denotes that it must either be selected from a list of system key-words or that it is identical to an item previously defined by the user.

f) item -- An item typed in all lower case letters is defined strictly by the user.

The formats for data sections 1 through 3 and 5 through 9 given in Ref. 2 are identical to those. Additional data for direct input of airfoil ordinates and slopes is required in Section 4, and this is described below. The additional data required for viscous calculations is given in Section 10, which follows.

4. Geometry Section

The following card formats for geometry data input should replace those given in Ref. 2.

19) FORMAT: [FUNCTIONAL, TABULAR], NASA

The airfoil section can be described by polynomials (FUNCTIONAL) or by a table of coordinates (TABULAR). If the functional format is chosen, polynomial coefficients and exponents from a suitable source, such as a least squares fit program may be entered. If the tabular option is chosen, ordinates and slopes must be defined at the aerodynamic mesh points (percent of local chord defined by the XI mesh definition given in Section 3), and may be provided by any suitable source (spline fit to measured data, for example). If the tabular option is chosen, the keyword NASA must be entered as written. The presence of this keyword allows for a future program enhancement.

If the FUNCTIONAL option is chosen, cards 20, and 21) as given in Section 4 of Ref. 2 are entered to defined the upper and lower surface polynomials. If the TABULAR option is chosen, cards 20A) and 21A) are required:

20A) UPPER: nzu, x_1,....x_{nzu}, z_1,....z_{nzu},
$dzdx_1$,....,$dzdx_{nzu}$

21A) LOWER: nzl, x_1,....x_{nzl}, z_1,....z_{nzl},
$dzdx_1$,....,$dzdx_{nzl}$

where nzu and nzl are the number of points defining the upper and lower surface of the airfoil. For the current implementation, this must be equal to the number of streamwise mesh points on the wing surface.

10. Viscous Calculation Section

The purpose of this section is to specify the Viscous Calculation option if the user so desires. If this option is not desired, then this section should be omitted.

1) BEGIN VISCOUS FLOW PARAMETERS

This data record is used to indicate that processing of data associated with the Viscous Calculation is to follow. The following card statements (2-5) are optional and need only be input if values other than the defaults are to be specified. Data records 2-4 define data associated with the viscous wedge (all values are nondimensional by local section chord).

2) (SHOCK OFFSET DISTANCE: xoffst)

Input of the shock offset distance.
The default is SHOCK OFFSET DISTANCE: .02.

3) (PRECURSOR LENGTH: xprec)

Input of the precursor length.
The default is PRECURSOR LENGTH: .02.

4) (RAMP LENGTH: xramp)

Input of the ramp length.
The default is RAMP LENGTH: 0.10.

5) (CALCULATION INTERVAL: iblcal)

Input of the viscous flow calculation update interval for both wedge and boundary-layer computations.
The default is CALCULATION INTERVAL: 1

6) BOUNDARY-LAYER SOLUTION

This data record is required if the boundary-layer calculation is to be executed and it also is the first data record associated with the boundary-layer calculation. The following card statements (7-11) are optional and need only be input if values other than the default values are to be input.

7) (PRINT INTERVAL: iblprt)

Input of the boundary-layer print interval.
The default is PRINT INTERVAL: 50.

8) (REYNOLDS NUMBER: reyinf)

Input of the free stream Reynolds number based on root chord.
The default is REYNOLDS NUMBER: 1.0E7

9) (TEMPERATURE: tinf)

Input of the free stream temperature (degrees Kelvin).
The default is TEMPERATURE: 300.0

10) (SUTHERLAND LAW CONSTANT: so)

Input of the Sutherland Law Constant (degrees Kelvin).
The default (defined for air) is SUTHERLAND LAW CONSTANT: 110.0.

11) (PRANDTL NUMBER: prt)

Input of the turbulent Prandtl number.
The default is PRANDTL NUMBER: 0.9

APPENDIX B

XTRAN3S SAMPLE PROBLEM

```
BEGIN PROBLEM DEFINITION SECTION
  TITLE: XTRAN3 BOUNDARY-LAYER VALIDATION (MBB-A3,AR=8.0,TR=0.4)
  STATIC ANALYSIS OF RIGID WING
  MACH NUMBER: 0.85
  FREE STREAM VELOCITY: 3000.
  RATIO OF SPECIFIC HEATS: 1.4
  TIME SCALING: 0.2
BEGIN COMPUTATIONAL CONTROL SECTION
  MAXIMUM STEADY ITERATIONS: 1800
  TIME DEPENDENT SOLUTION: HIGH FREQUENCY
  MODIFIED EQUATION FORM: AMES
  INTEGRATOR STEP SIZE: 0.0034906585
BEGIN COMPUTATIONAL GRID SECTION
  BEGIN XI MESH DEFINITION
    MESH NAME: XIMESH
    MESH SOURCE: TABLE
    NUMBER OF UPSTREAM MESHPOINTS: 11
    NUMBER OF DOWNSTREAM MESHPOINTS: 10
    TOTAL NUMBER OF MESHPOINTS: 60
  BEGIN ETA MESH DEFINITION
    MESH NAME: ETAMESH
    MESH SOURCE: INPUT
    NUMBER OF INBOARD MESHPOINTS: 13
    NUMBER OF OUTBOARD MESHPOINTS: 7
    ARRAY OF ETA MESH POINTS
    -0.25,0.00,0.25,0.50,0.75,1.00,1.30,1.70,2.00,2.25,      +
     2.50,2.65,2.75,2.80,2.90,3.05,3.30,3.80,4.30,5.30
  BEGIN Z MESH DEFINITION
    MESH NAME: ZMESH
    MESH SOURCE: TABLE
    NUMBER OF MESHPOINTS ABOVE WING: 20
    NUMBER OF MESHPOINTS BELOW WING: 20
BEGIN GEOMETRY SECTION
  WING PLANFORM DESCRIPTION
    FORMAT OF PLANFORM DATA: RATIO
    ASPECT RATIO: 8.0
    TAPER RATIO: 0.4
    SWEEP ANGLE: 30.0
  REFERENCE AREA: 1.939
    MEAN AERODYNAMIC CHORD: 1.0
    TOTAL MOMENT CENTER REFERENCE: 0.0
    REFERENCE CHORD: 1.0
```

```
   AIRFOIL SECTION LIBRARY
     SECTION: MBB-A3,UPPER/LOWER
     DIMENSION: CHORDWISE,NO,VERTICAL,NO
     FORMAT : TABULAR,NASA
       UPPER :39,.005,.015,.025,.035,.045,.060,.080,.100,.130,.160,.190, +
              .220,.250,.280,.310,.340,.370,.400,.430,.460,.490,.520,.550,+
              .580,.610,.640,.670,.700,.730,.760,.790,.820,.850,.880,.910,+
              .935,.960,.980,1.000,                                       +
              .0075,.0131,.0169,.0199,.0226,.0259,.0297,.0329,.0369,.0402,+
              .0428,.0450,.0466,.0479,.0488,.0493,.0495,.0493,.0489,.0481,+
       .0471,.0458,.0443,.0426,.0406,.0384,.0360,.0334,.0306,.0277,.0246,+
              .0214,.0181,.0146,.0111,.0081,.0050,.0025,.0000,            +
              .7564,.4359,.3355,.2809,.2448,.2074,.1732,.1483,.1200,.0979,+
              .0793,.0631,.0486,.0353,.0229,.0114,.0004,-.0099,-.0198,    +
              -.0291,-.0381,-.0466,-.0547,-.0624,-.0697,-.0766,-.0831,    +
       -.0892,-.0949,-.1002,-.1050,-.1094,-.1133,-.1167,-.1197,-.1218,    +
              -.1235,-.1247,-.1256
       LOWER :39,.005,.015,.025,.035,.045,.060,.080,.100,.130,.160,.190, +
              .220,.250,.280,.310,.340,.370,.400,.430,.460,.490,.520,.550,+
              .580,.610,.640,.670,.700,.730,.760,.790,.820,.850,.880,.910,+
              .935,.960,.980,1.000,                                       +
              -.0064,-.0099,-.0117,-.0129,-.0139,-.0149,-.0160,-.0169,    +
              -.0181,-.0193,-.0206,-.0218,-.0230,-.0240,-.0250,-.0258,    +
              -.0263, -.0266,-.0266,-.0264,-.0258,-.0249,-.0237,-.0223,   +
              -.0205,-.0185,-.0164,-.0141,-.0117,-.0092,-.0068,-.0046,    +
              -.0026,-.0009,.0003,.0009,.0010,.0007,.0000,                +
              -.5395,-.2329,-.1459,-.1042,-.0805,-.0607,-.0482,-.0430,    +
              -.0408,-.0408,-.0409,-.0400,-.0378,-.0340,-.0288,-.0222,    +
              -.0144,-.0056,.0039,.0139,.0242,.0344,.0444,.0537,.0621,    +
              .0693,.0751,.0791,.0810,.0805,.0774,.0712,.0618,.0488,      +
              .0319,.0146,-.0058,-.0244,-.0453
   STATION COUNT: 2,NONDIMENSIONAL
     LOCATION: 0.0
     NAME: MBB-A3
     LOCATION: 2.77
     NAME: MBB-A3
BEGIN BOUNDARY CONDITION SECTION
  LIFTING SURFACE BOUNDARY CONDITION: STEADY
    ANGLE OF ATTACK: 1.0 DEGREES
  WAKE BOUNDARY CONDITION: STEADY
  DOWNSTREAM BOUNDARY CONDITION: STEADY
BEGIN VISCOS FLOW PARAMETERS
  SHOCK OFFSET DISTANCE:0.02
  PRECURSOR LENGTH :0.02
  RAMP LENGTH:0.10
  CALCULATION INTERVAL:1
  BOUNDARY-LAYER SOLUTION
    PRINT INTERVAL:450
    REYNOLDS NUMBER:1.0E7
    TEMPERATURE:300.0
    SUTHERLAND LAW CONSTANT:110.0
    PRANDTL NUMBER:0.9
BEGIN CHECKPOINT-RESTART SECTION
  RESTART : YES
  SAVE FREQUENCY: 900
BEGIN POST-PROCESSING SECTION
  PRINT GEOMETRY
  PRINT COMPUTATIONAL MESH
  PRINT PRESSURE DISTRIBUTION :2,3,4,5,6,7,8,9,10,11,12,13
  PRINT AERODYNAMIC COEFFICIENTS
  TIME HISTORY REPORTING FREQUENCY : 450
END OF PROBLEM
/EOF
```

REFERENCES

1. Borland, C. J. and Rizzetta, D. P., "Transonic Unsteady Aerodynamics for Aeroelastic Applications--Vol I: Technical Development Summary," AFFWAL TR-80-3107, Vol. I, June 1982.

2. Borland, C. J., Thorne, R. G., and Yeagley, L. R., "Transonic Unsteady Aerodynamics for Aeroelastic Application--Vol. II: User's Manual," AFFWAL TR-80-3107, Vol. II, June 1982.

3. Thorne, R. G. and Yeagley, L. R., "Transonic Unsteady Aerodynamics for Aeroelastic Applications--Vol. III: Programmer's Manual," AFFWAL TR-80-3107, Vol. III, June 1982.

4. Rizzetta, D. P. and Borland, C. J., "Numerical Solution of Three-Dimensional Unsteady Transonic Flow Over Wings Including Inviscid/Viscous Interactions" Final Report, NASA CR-166561, August, 1982.

5. Green, J. E., "Application of Head's Entrainment Method to the Prediction of Turbulent Boundary Layers and Wakes in Compressible Flow," RAE Reports and Memoranda No. 3788, April 1972.

6. Control Data Corporation, "UPDATE Version 1 Reference Manual," CDC Document 60449900, Rev. C, 1980.

7. Edwards, J. W., Bennett, R. M., Whitlow, W., Jr., and Seidel, D. A. "Time-Marching Transonic Flutter Solutions Including Angle-of-Attack Effects," AIAA Paper 82-3685, 23rd Structures Structural Dynamics, and Materals Conference, New Orleans, May 10-12, 1982.

8. Lambiotte, J. J., Jr., "An Alternating Direction Implicit Method for the Control Data STAR-100 Vector Computer, NASA TP 1282, September, 1978.

9. Calahan, D. A., Ames, W. G., and Sesck, E. J., "A Collection of Equation Solving Codes for the CRAY-1" SEL Report No. 133, University of Michigan, August, 1979.

10. Tijdeman, H. et al, "Transonic Wind Tunnel Test on an Oscillating Wing with External Stores; Part II The Clean Wing" AFFDL TR-78-194, Part II, March, 1979.

11. Borland, C. J. and Rizzetta, D. P., "Nonlinear Transonic Flutter Analysis," AIAA Journal Vol. 20, No. 11, Nov. 1982, p 1606-1615.

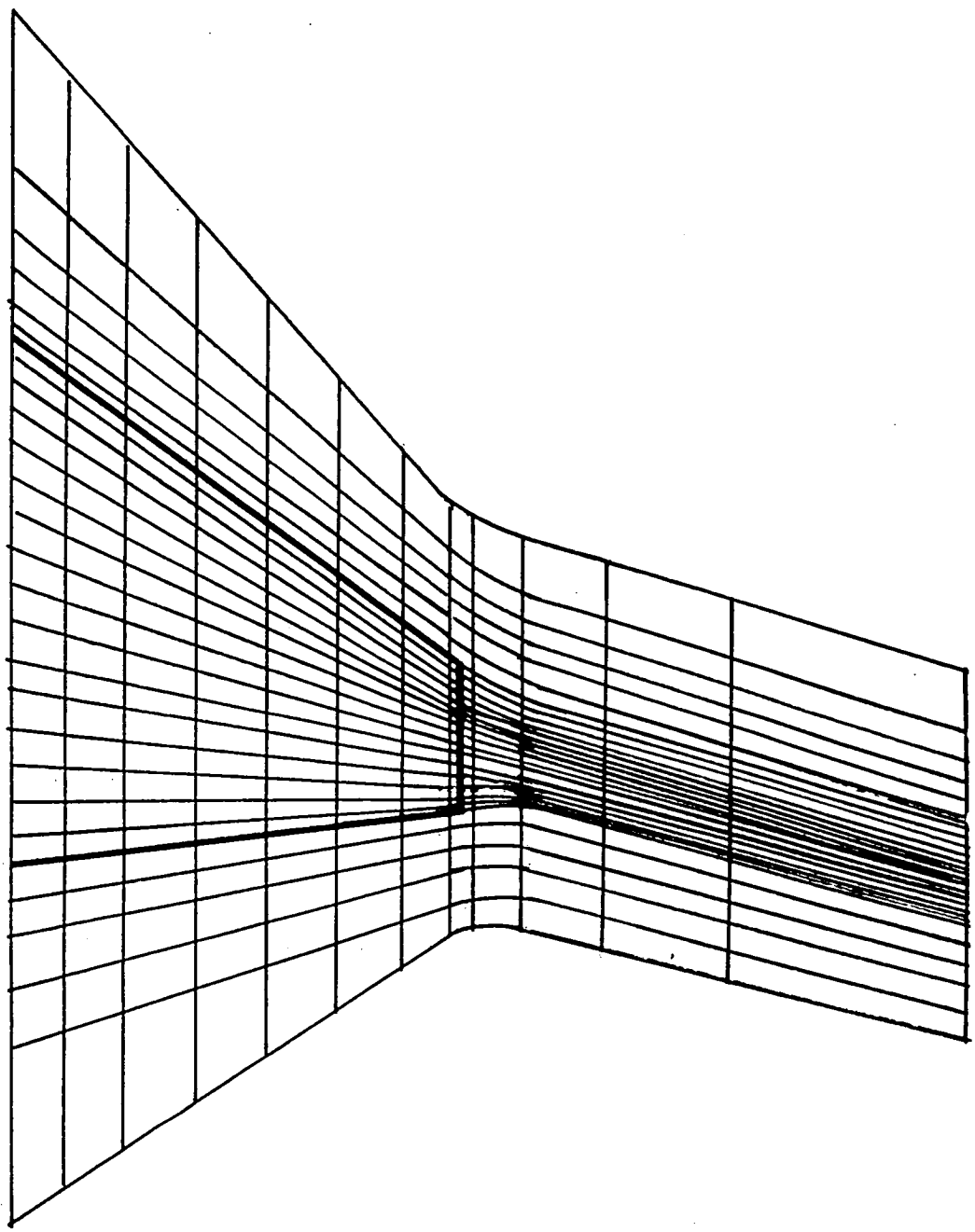

Figure 1. XTRAN3S Grid -- Original Mesh Transformation

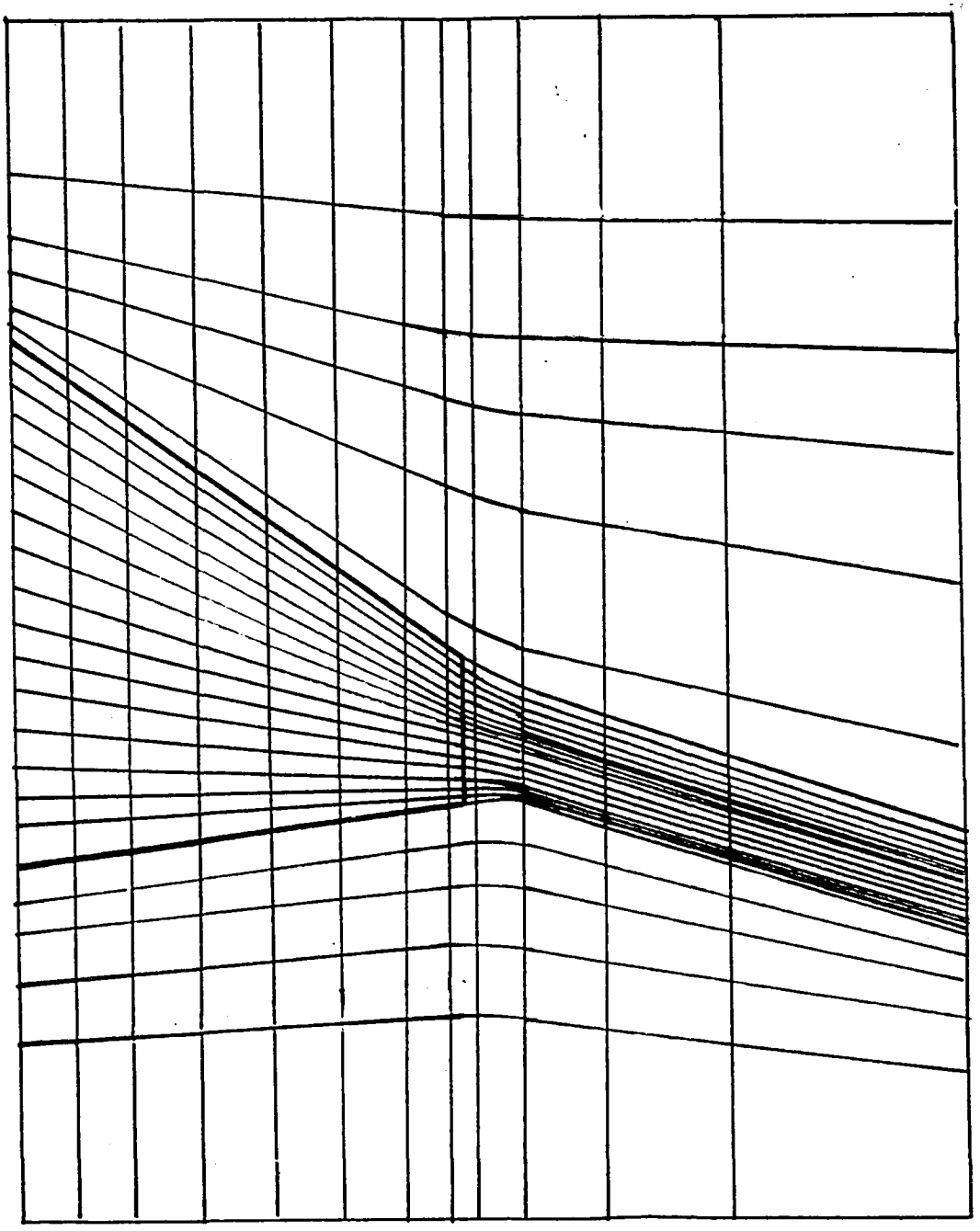

Figure 2. XTRAN3S Grid – Modified Mesh Transformation

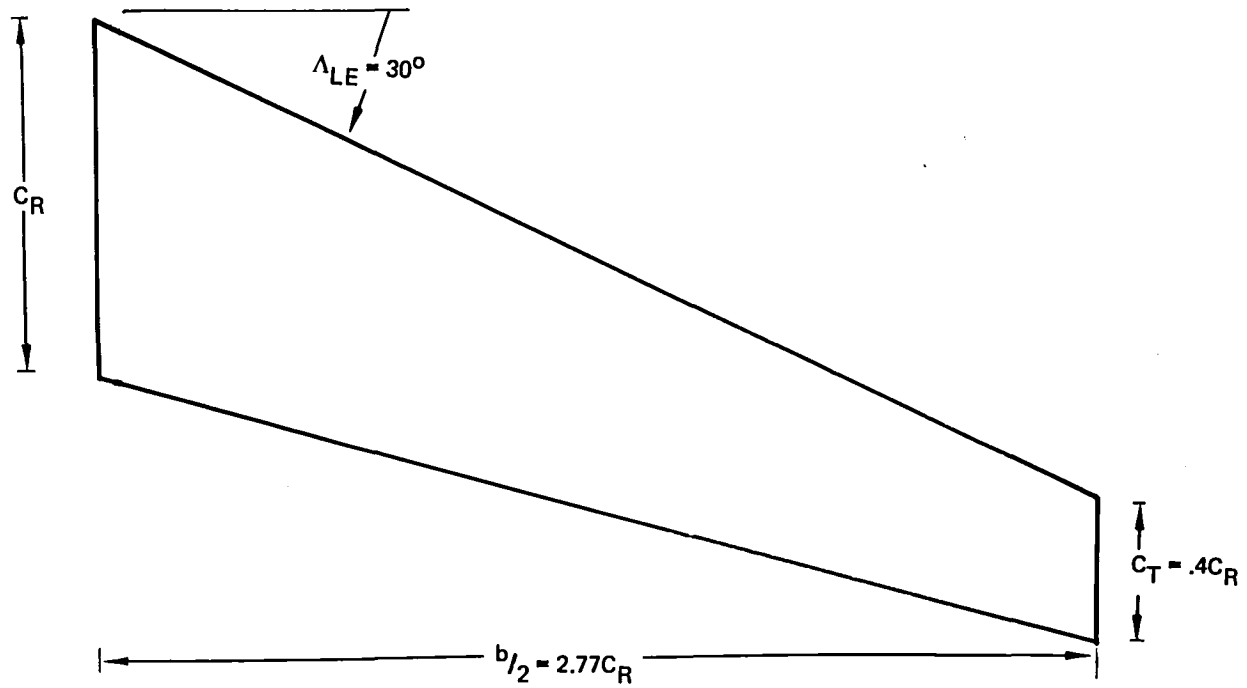

Figure 3a. Typical Transport Wing Planform

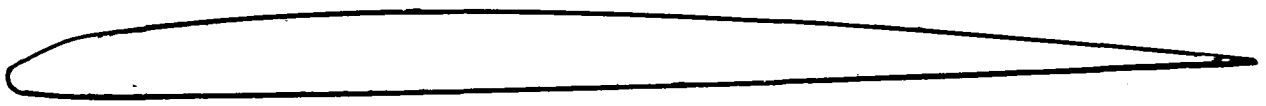

Figure 3b. MBB-A3 Airfoil Section

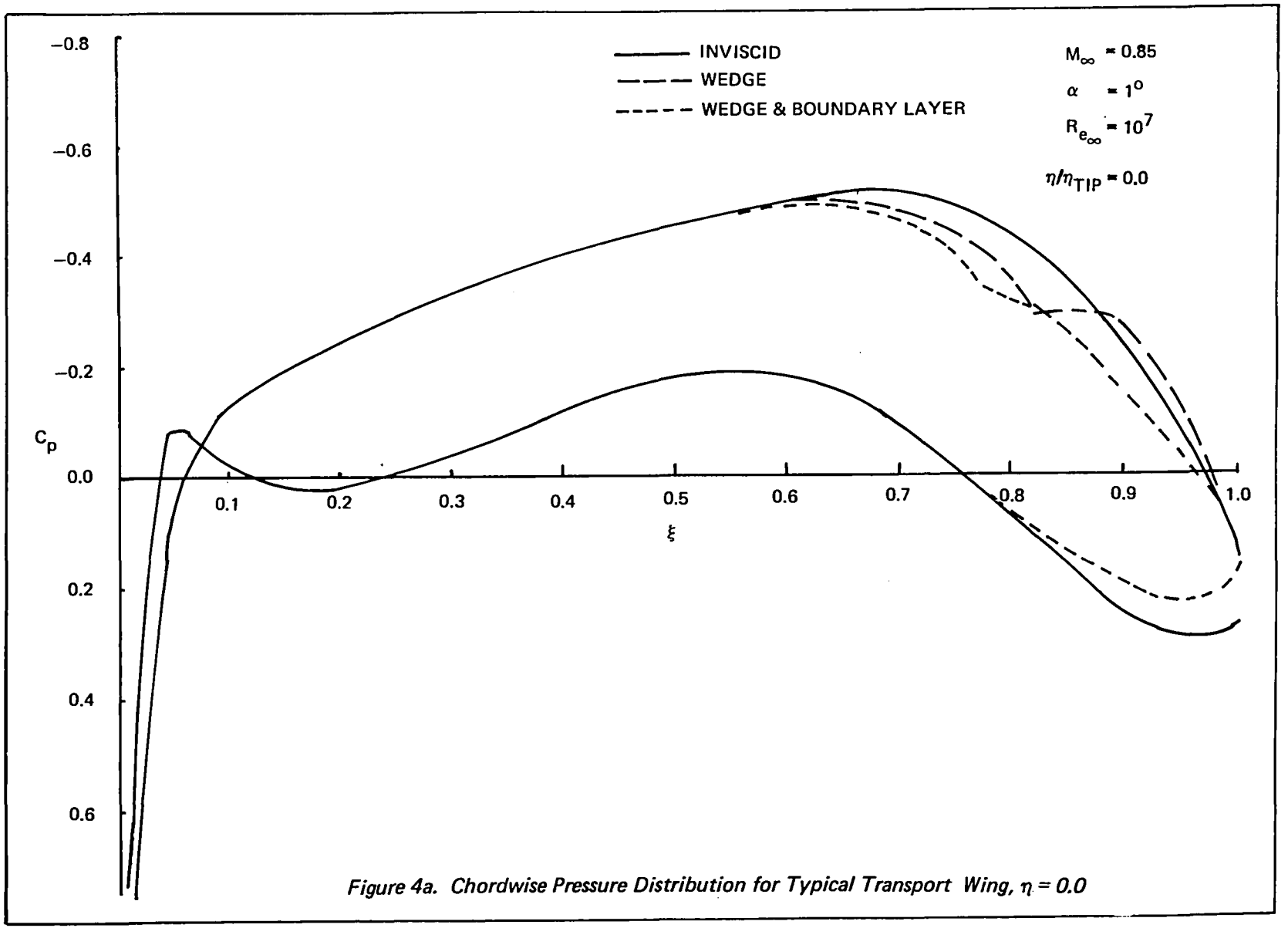

Figure 4a. Chordwise Pressure Distribution for Typical Transport Wing, $\eta = 0.0$

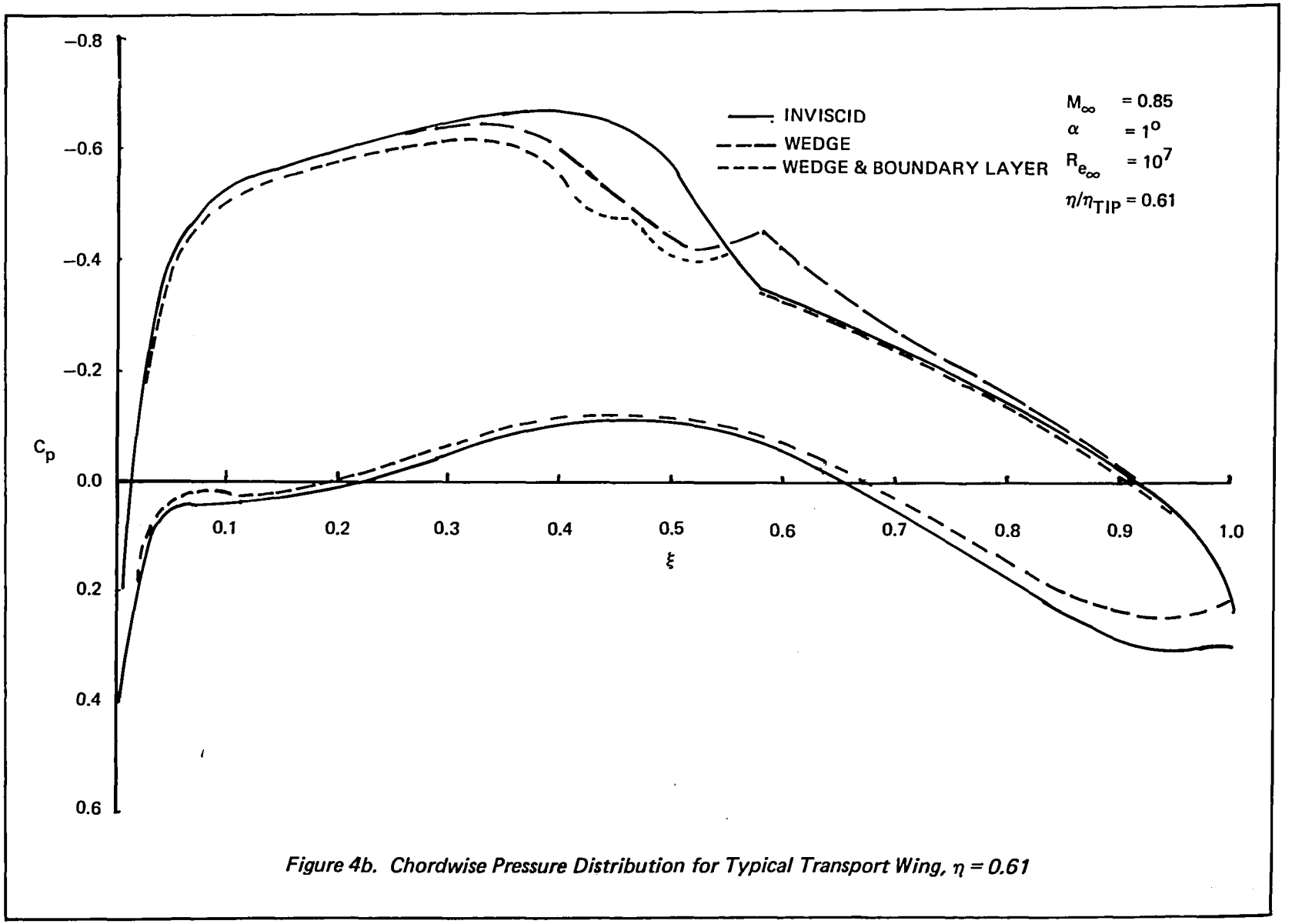

Figure 4b. Chordwise Pressure Distribution for Typical Transport Wing, $\eta = 0.61$

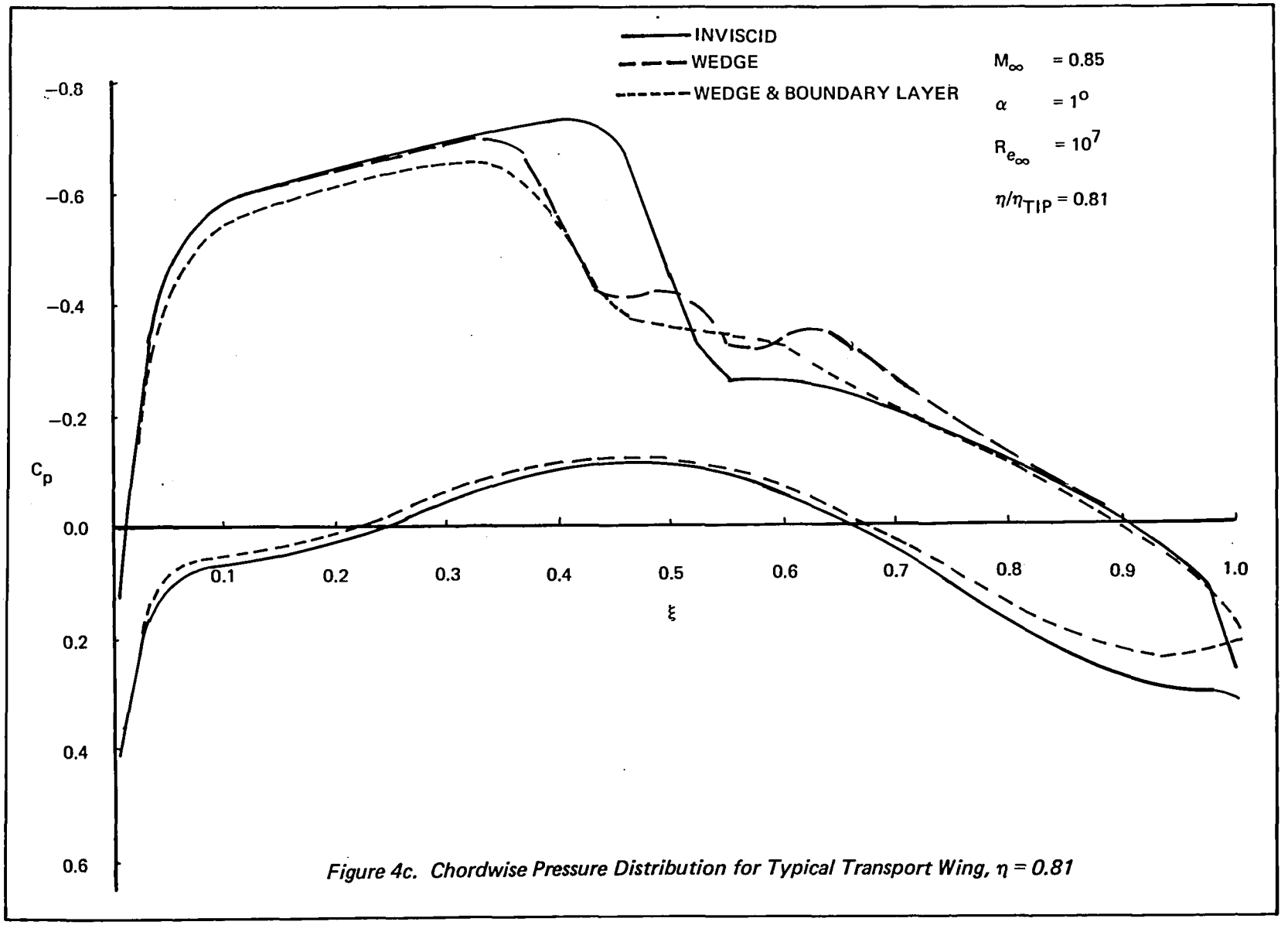

Figure 4c. Chordwise Pressure Distribution for Typical Transport Wing, $\eta = 0.81$

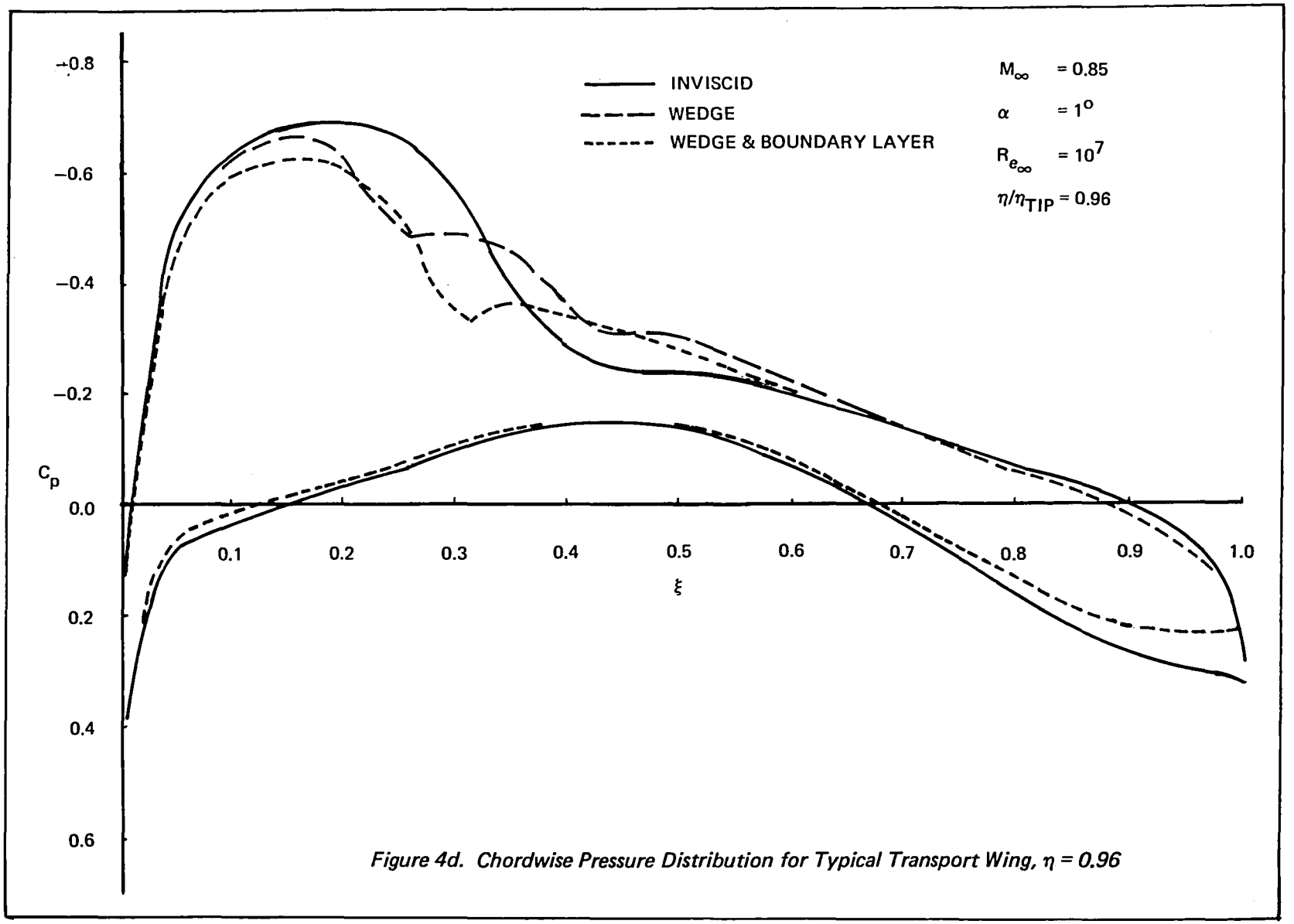

Figure 4d. Chordwise Pressure Distribution for Typical Transport Wing, η = 0.96

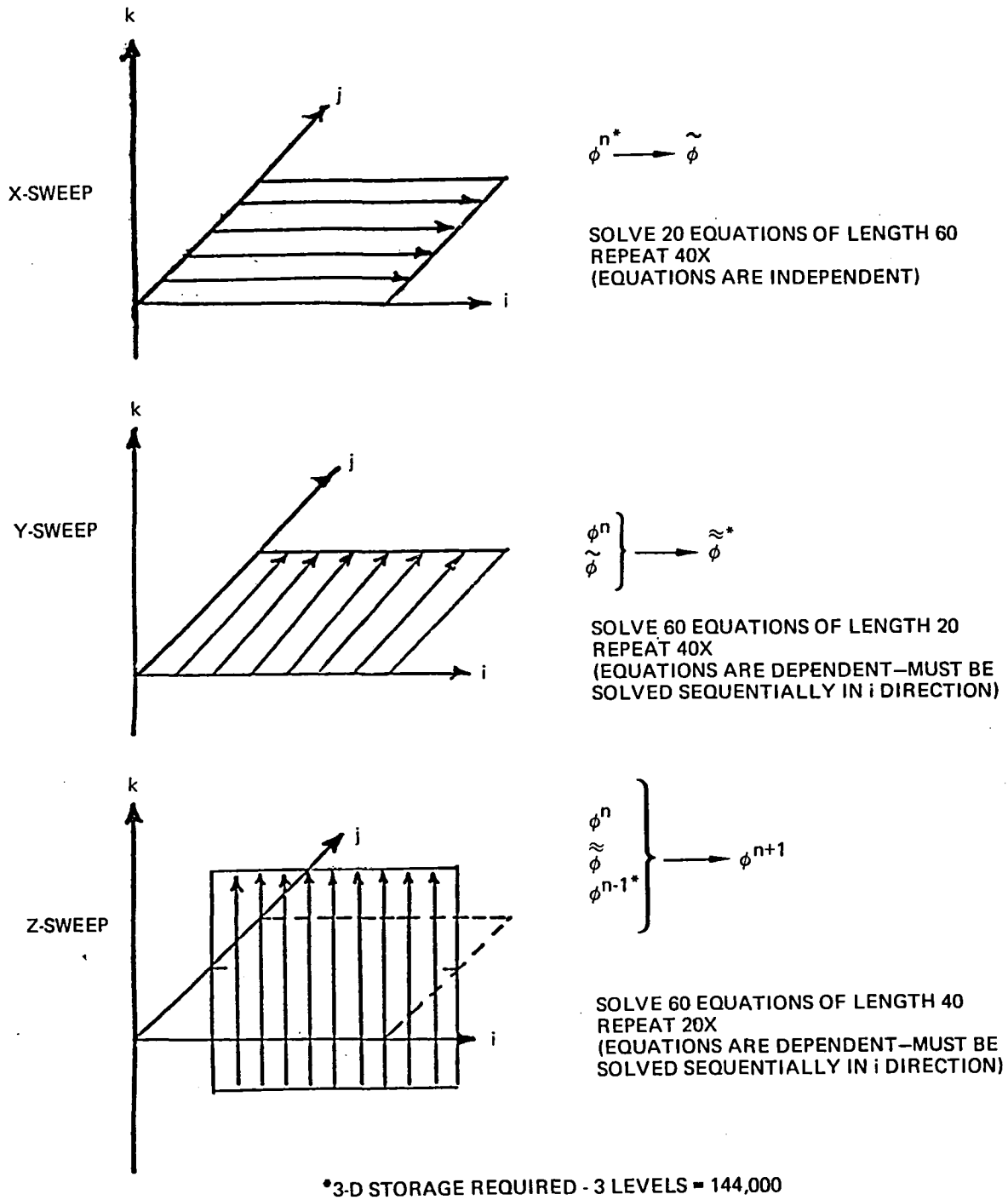

Figure 5. Original Algorithm Storage Scheme

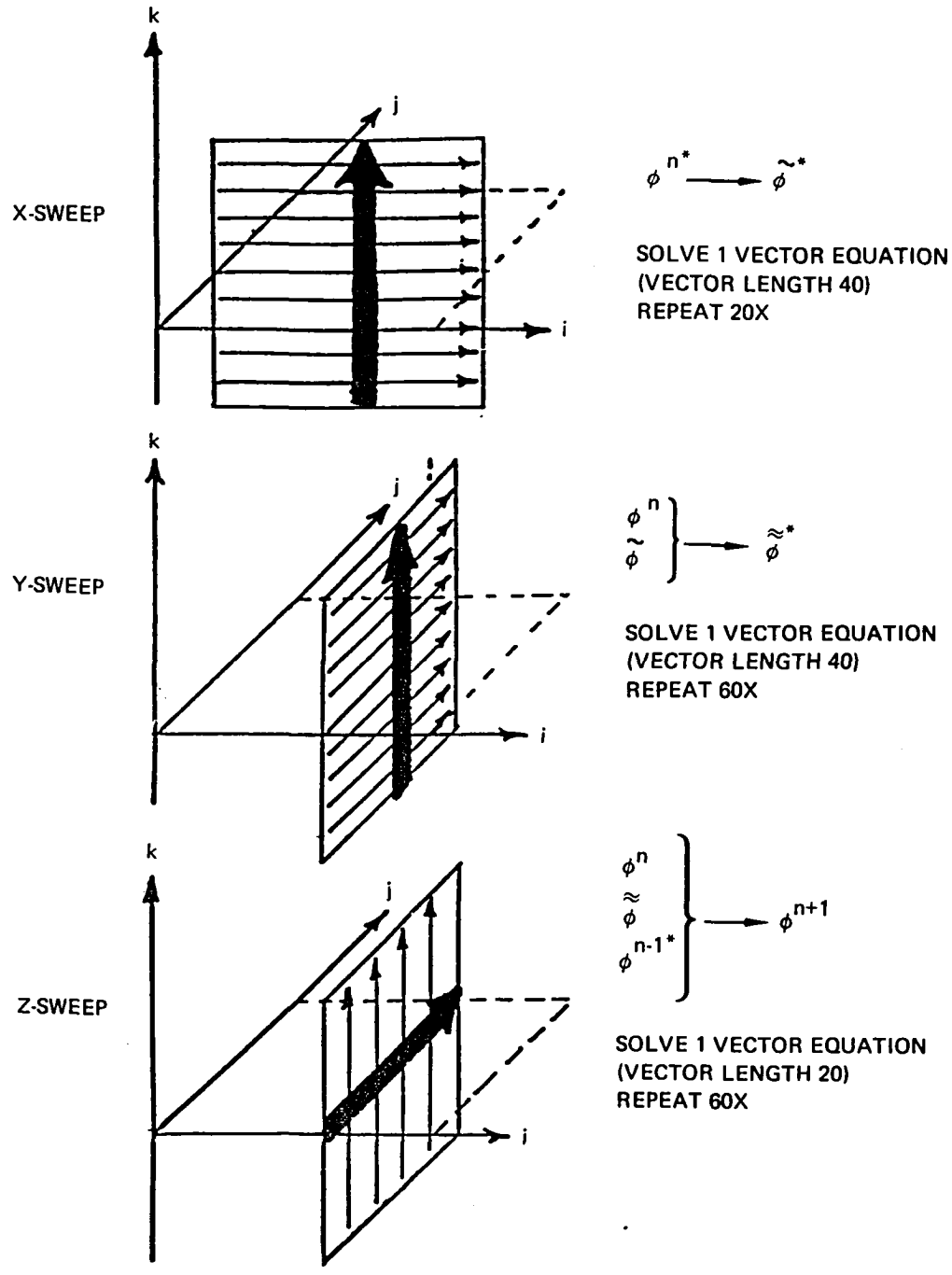

*3-D STORAGE REQUIRED - 4 LEVELS + 9 COEFFICIENTS = 624,000

Figure 6. Modified Algorithm Storage Scheme

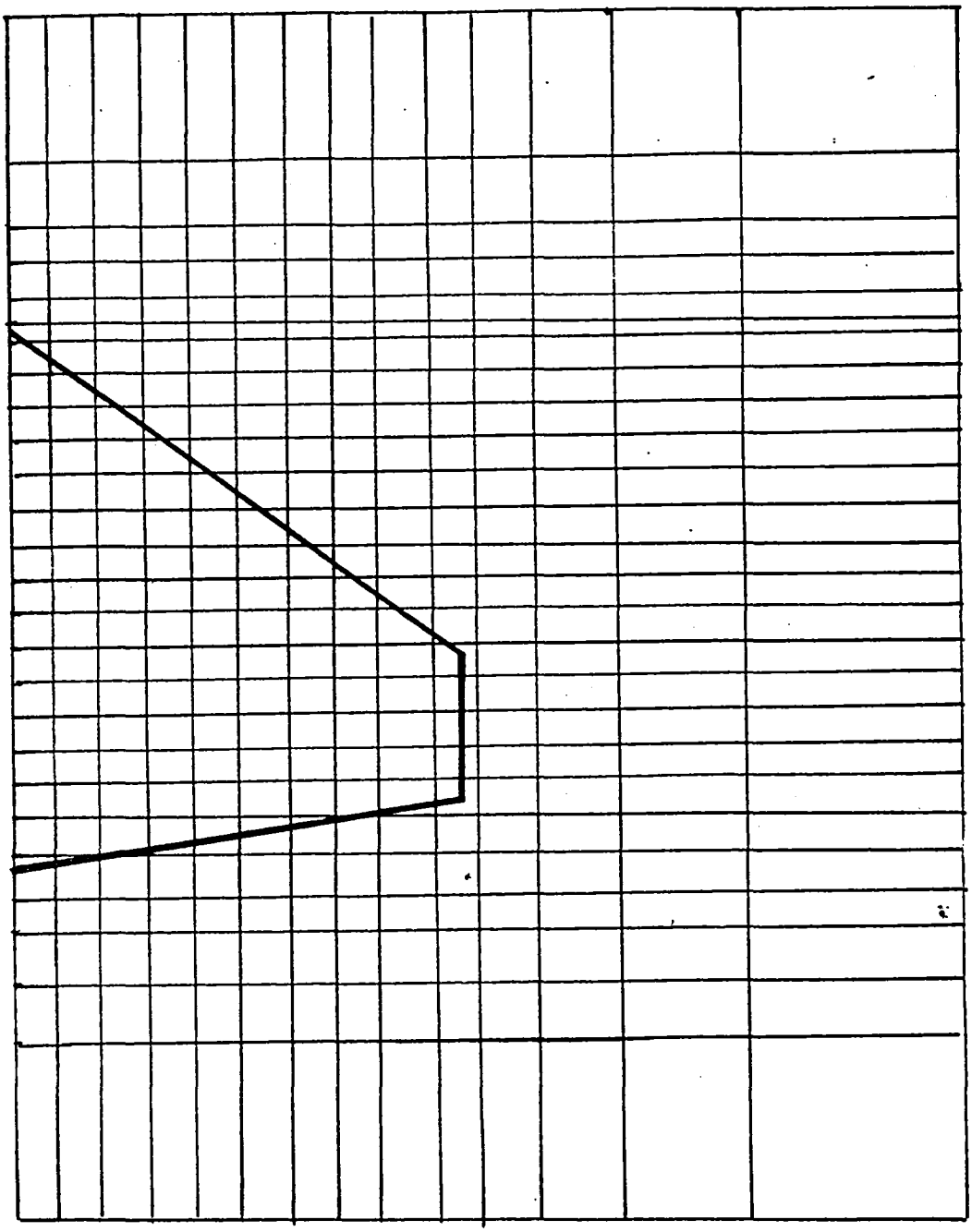

Figure 7. XTRAN3S Grid — Cartesian Mesh

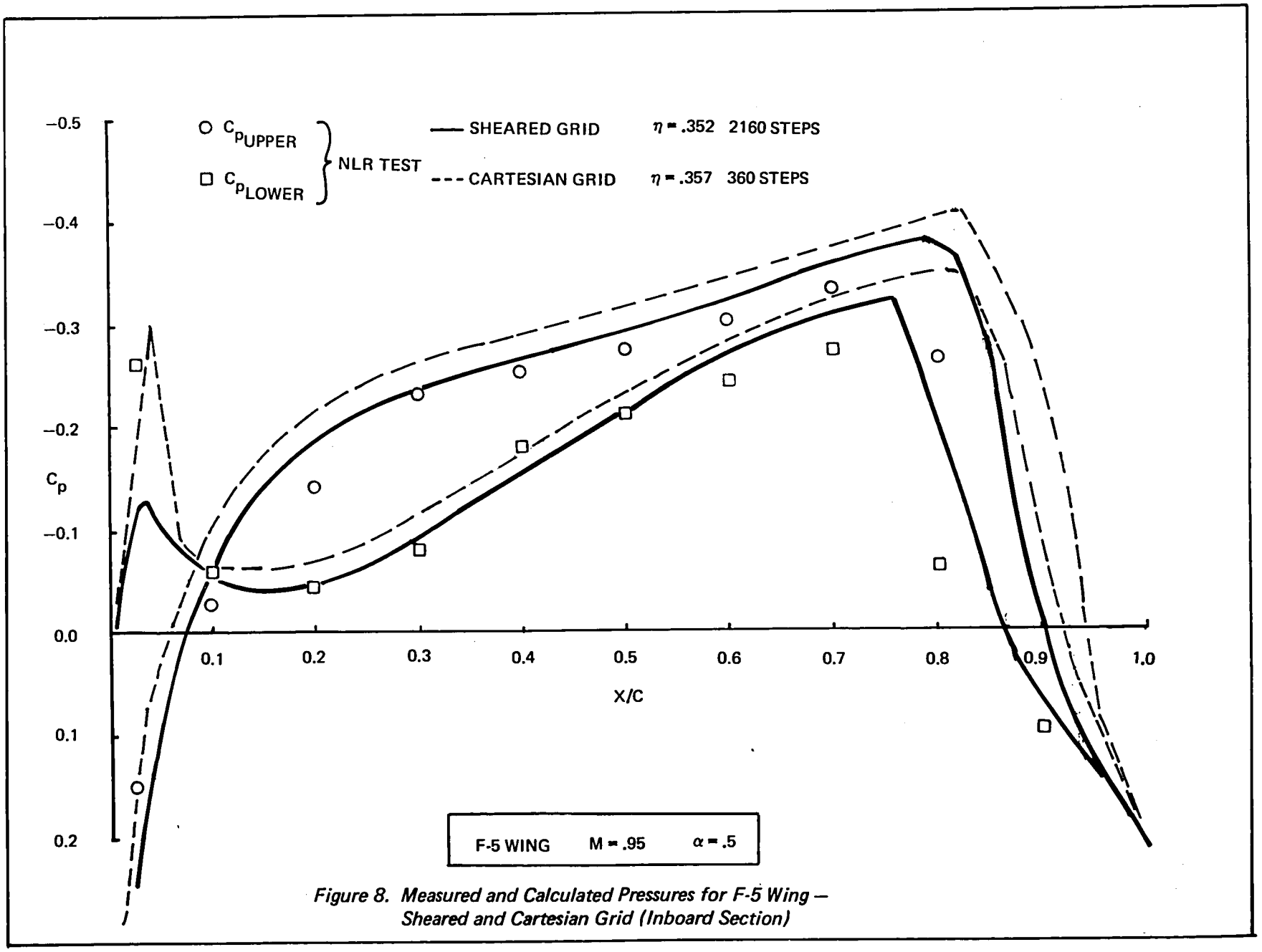

Figure 8. Measured and Calculated Pressures for F-5 Wing — Sheared and Cartesian Grid (Inboard Section)

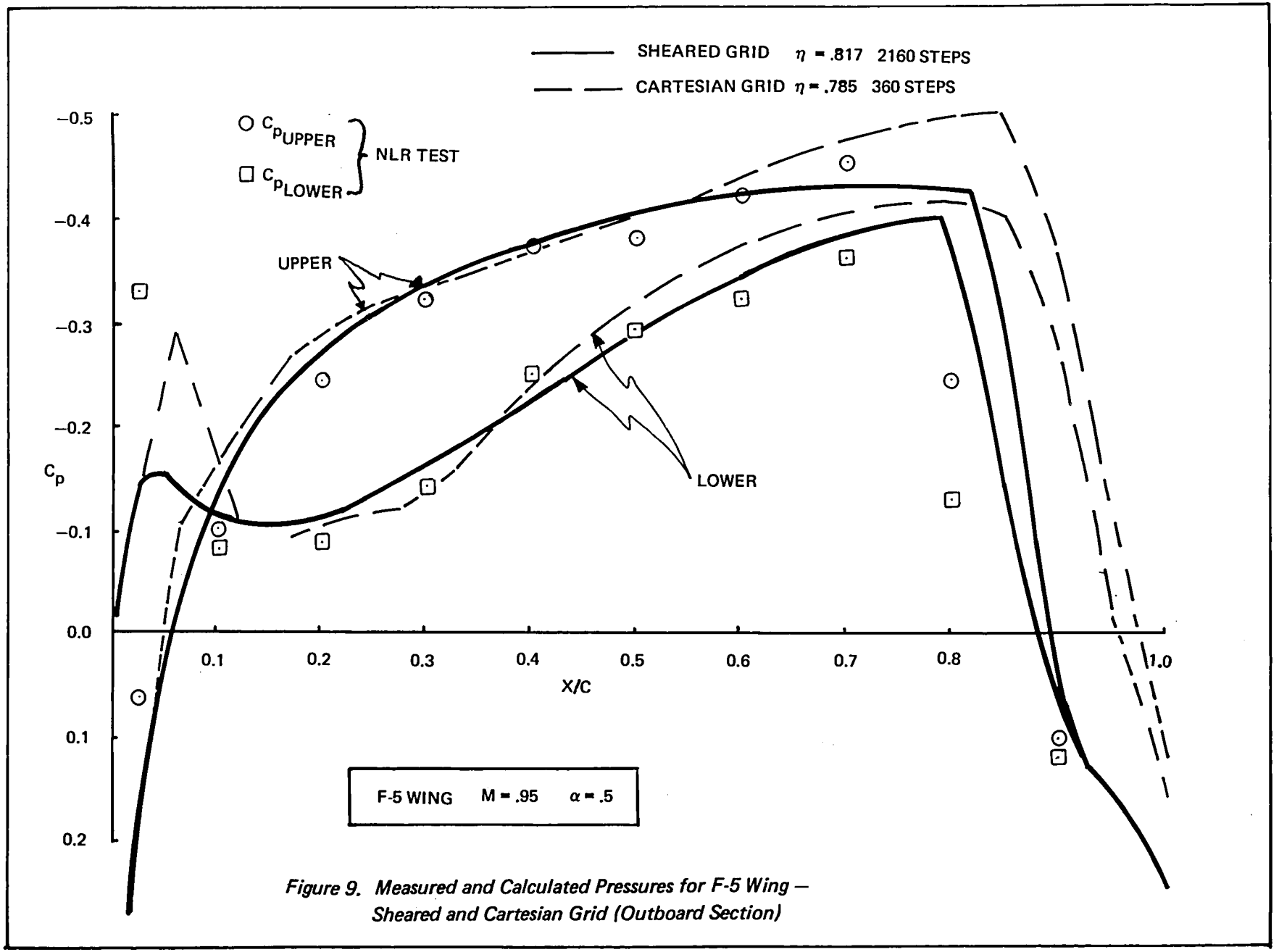

Figure 9. Measured and Calculated Pressures for F-5 Wing — Sheared and Cartesian Grid (Outboard Section)

DO NOT REMOVE SLIP FROM MATERIAL

Delete your name from this slip when returning material to the library.

NAME	MS
Chu, Li	173

NASA Langley (Rev. May 1988) RIAD N-75